



RESEARCH

Open Access



# Dapagliflozin mitigates cellular stress and inflammation through PI3K/AKT pathway modulation in cardiomyocytes, aortic endothelial cells, and stem cell-derived $\beta$ cells

Fatmah R. Alsereidi<sup>1,2,3</sup> , Zenith Khashim<sup>2</sup>, Hezlin Marzook<sup>1</sup>, Ahmed M. Al-Rawi<sup>1</sup>, Tiana Salomon<sup>2</sup>, Mahra K. Almansoori<sup>4</sup>, Moustafa M. Madkour<sup>1</sup>, Ahmed Mohamed Hamam<sup>5</sup>, Mahmoud M. Ramadan<sup>1,6,7</sup>, Quinn P. Peterson<sup>2,8</sup> and Mohamed A. Saleh<sup>1,6,9\*</sup> 

## Abstract

**Abstract** Dapagliflozin (DAPA), a sodium-glucose cotransporter 2 (SGLT2) inhibitor, is well-recognized for its therapeutic benefits in type 2 diabetes (T2D) and cardiovascular diseases. In this comprehensive in vitro study, we investigated DAPA's effects on cardiomyocytes, aortic endothelial cells (AECs), and stem cell-derived beta cells (SC- $\beta$ ), focusing on its impact on hypertrophy, inflammation, and cellular stress. Our results demonstrate that DAPA effectively attenuates isoproterenol (ISO)-induced hypertrophy in cardiomyocytes, reducing cell size and improving cellular structure. Mechanistically, DAPA mitigates reactive oxygen species (ROS) production and inflammation by activating the AKT pathway, which influences downstream markers of fibrosis, hypertrophy, and inflammation. Additionally, DAPA's modulation of SGLT2, the Na<sup>+</sup>/H<sup>+</sup> exchanger 1 (NHE1), and glucose transporter (GLUT 1) type 1 highlights its critical role in maintaining cellular ion balance and glucose metabolism, providing insights into its cardioprotective mechanisms. In aortic endothelial cells (AECs), DAPA exhibited notable anti-inflammatory properties by restoring AKT and phosphoinositide 3-kinase (PI3K) expression, enhancing mitogen-activated protein kinase (MAPK) activation, and downregulating inflammatory cytokines at both the gene and protein levels. Furthermore, DAPA alleviated tumor necrosis factor (TNF $\alpha$ )-induced inflammation and stress responses while enhancing endothelial nitric oxide synthase (eNOS) expression, suggesting its potential to preserve vascular function and improve endothelial health. Investigating SC- $\beta$  cells, we found that DAPA enhances insulin functionality without altering cell identity, indicating potential benefits for diabetes management. DAPA also upregulated MAFA, PI3K, and NRF2 expression, positively influencing  $\beta$ -cell function and stress response. Additionally, it attenuated NLRP3 activation in inflammation and reduced NHE1 and glucose-regulated protein GRP78 expression, offering novel insights into its anti-inflammatory and stress-modulating effects. Overall, our findings elucidate the multifaceted therapeutic potential of DAPA across various cellular models, emphasizing its role in mitigating hypertrophy, inflammation, and cellular stress through the

\*Correspondence:  
Mohamed A. Saleh  
mohamed.saleh@sharjah.ac.ae

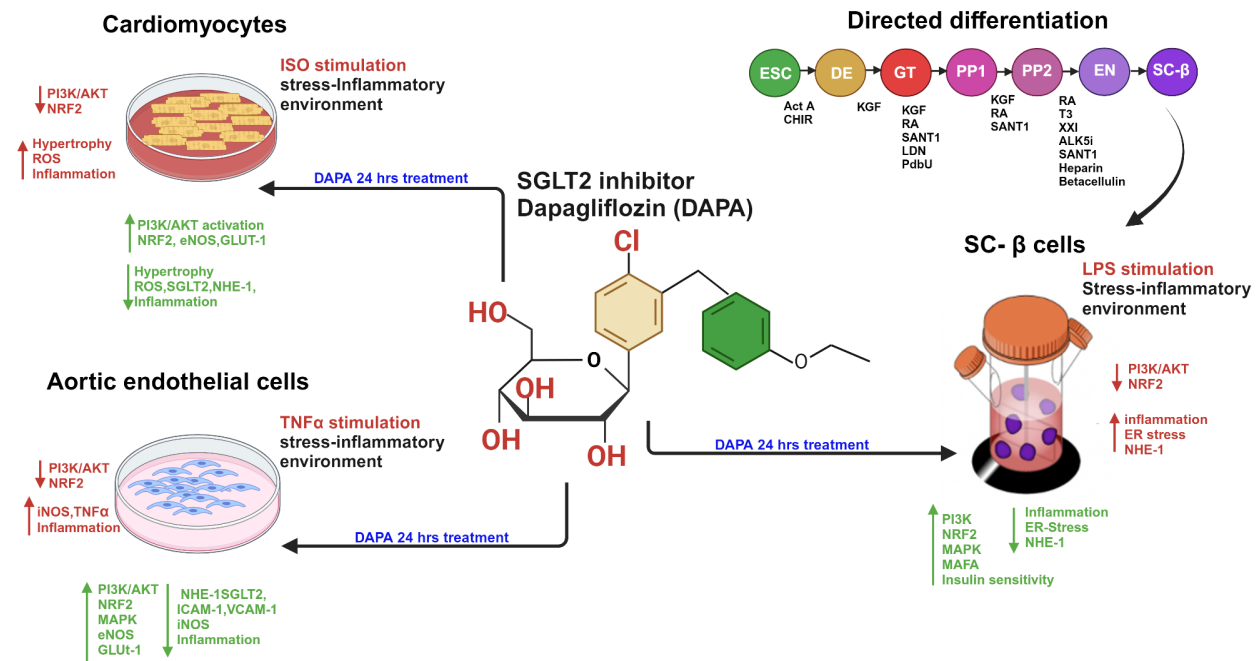
Full list of author information is available at the end of the article



© The Author(s) 2024. **Open Access** This article is licensed under a Creative Commons Attribution-NonCommercial-NoDerivatives 4.0 International License, which permits any non-commercial use, sharing, distribution and reproduction in any medium or format, as long as you give appropriate credit to the original author(s) and the source, provide a link to the Creative Commons licence, and indicate if you modified the licensed material. You do not have permission under this licence to share adapted material derived from this article or parts of it. The images or other third party material in this article are included in the article's Creative Commons licence, unless indicated otherwise in a credit line to the material. If material is not included in the article's Creative Commons licence and your intended use is not permitted by statutory regulation or exceeds the permitted use, you will need to obtain permission directly from the copyright holder. To view a copy of this licence, visit <http://creativecommons.org/licenses/by-nc-nd/4.0/>.

activation of the AKT pathway and other signaling cascades. These mechanisms may not only contribute to enhanced cardiac and endothelial function but also underscore DAPA's potential to address metabolic dysregulation in T2D.

**Graphical abstract**



**Key message**

- 1.DAPA effectively attenuates ISO-induced cardiomyocyte hypertrophy by reducing cell size and improving cellular structure.
- 2.DAPA exhibits anti-inflammatory properties in AECs by restoring AKT and PI3K expression, upregulating MAPK activation, and downregulating inflammatory gene expression.
- 3.DAPA enhances insulin functionality in SC-β cells without altering cell identity, suggesting potential benefits in diabetes management.
- 4.DAPA's modulation of SGLT2, NHE1, and GLUT1 expression in cardiomyocytes underscores its role in cellular ion balance and glucose metabolism, contributing to its cardioprotective mechanisms.
- 5.DAPA alleviates TNFα-induced inflammation and stress responses in AECs, while enhancing eNOS expression, indicating its potential to preserve vascular function.
- 6.DAPA attenuates NLRP3 activation and reduces NHE1 and GRP78 expression in SC-β cells, offering novel insights into its anti-inflammatory and stress-modulating effects.

**Keywords** Dapagliflozin, Sodium-glucose cotransporter, Cardiomyocyte, Inflammation, AKT signaling, Endothelial cells, Beta cells

**Introduction**

Cardiomyocyte hypertrophy is a cellular response characterized by an increase in cell size, often resulting from mechanical stress or neurohumoral stimulation, such as that induced by isoproterenol (ISO), a synthetic catecholamine and β-adrenergic receptor agonist [1–3]. While hypertrophy is typically a consequence of underlying cardiovascular diseases, it exacerbates cardiac conditions by impairing cardiac function and heightening the risk of

adverse cardiovascular events [4, 5]. Understanding the molecular mechanisms and potential therapeutic interventions that can mitigate cardiomyocyte hypertrophy is crucial for developing strategies to improve cardiovascular outcomes [4, 5].

Dapagliflozin (DAPA), an inhibitor of sodium-glucose cotransporter2 (SGLT2), has gained attention for its cardiovascular benefits beyond its primary function in managing hyperglycemia in patients with type 2 diabetes

mellitus (T2DM). Clinical studies have highlighted significant cardiovascular advantages associated with DAPA treatment, including reduced incidences of heart failure and cardiovascular mortality, regardless of its glucose-lowering effects. Although the precise mechanisms underlying DAPA's cardioprotective effects remain partially understood, preclinical studies have provided valuable insights into its potential modes of action [6–8].

Stimuli like ISO trigger increased production of reactive oxygen species (ROS) and inflammation, both pivotal in developing and progressing cardiac hypertrophy. The AKT signaling pathway, a crucial regulator of cell growth, survival, and metabolism, plays a central role in controlling ROS production, hypertrophy, fibrosis, and inflammation. Activating AKT boosts the activity of antioxidant enzymes and mitochondrial function, thereby reducing oxidative stress. Additionally, it regulates protein synthesis and inflammatory responses, contributing to the mitigation of cardiac hypertrophy and fibrosis [9–12]. The AKT pathway commences with the binding of growth factors or insulin to their respective receptors on the cell surface, initiating the activation of phosphoinositide 3-kinase (PI3K). PI3K generates phosphatidylinositol-3,4,5-trisphosphate (PIP3), which recruits AKT to the plasma membrane for activation through phosphorylation by 3'-phosphoinositide dependent kinase (PDK)1 and mTORC2. Once activated, AKT phosphorylates a broad range of substrates involved in processes like glucose metabolism, protein synthesis, and cell survival [13, 14]. Several studies have emphasized the cardioprotective properties of DAPA, frequently attributing them to DAPA's modulation of the AKT pathway [15]. The activation of the AKT pathway is increasingly acknowledged as a pivotal mechanism through which DAPA can inhibit cardiomyocyte hypertrophy.

Emerging evidence suggests that DAPA may confer beneficial effects on vascular endothelial cells. Endothelial dysfunction and inflammation are central drivers of atherosclerosis and cardiovascular disease [16, 17]. DAPA's potential to alleviate endothelial dysfunction and inflammation could significantly contribute to its cardiovascular protective effects. AECs play a pivotal role in vascular homeostasis and blood pressure regulation [10, 12, 15]. AECs dysfunction is a hallmark of various cardiovascular diseases, including atherosclerosis and hypertension. SGLT2 inhibitors like DAPA have demonstrated improvements in endothelial function, possibly by reducing oxidative stress and inflammation [18, 19]. This enhancement in endothelial function is critical, as healthy AECs are vital for maintaining vascular tone and integrity, consequently lowering the risk of cardiovascular events.

While it's established that SGLT2 is typically not expressed in pancreatic  $\beta$ -cells, recent studies suggest

that DAPA may still affect  $\beta$ -cell function and survival through indirect or off-target mechanisms [20–22]. Understanding the direct impact of DAPA on  $\beta$ -cells could shed light on its role in managing both diabetes and cardiovascular diseases. SGLT2 inhibitors not only reduce blood glucose levels by preventing glucose reabsorption in the kidneys but may also provide protective effects on  $\beta$ -cells. By mitigating glucotoxicity, these agents help preserve  $\beta$ -cell function and slow the progression of diabetes. This dual benefit of glycemic control and  $\beta$ -cell preservation underscores the importance of DAPA as a pivotal therapeutic agent in the comprehensive management of T2DM [23].

Therefore, in our current study, we aim to study the diverse roles of DAPA in cardiac protection, improving vascular health, and supporting  $\beta$ -cell function, providing valuable insights into its potential therapeutic uses in cardiovascular diseases. Our study focuses on how DAPA influences cardiomyocytes, AECs, and SC- $\beta$  cells when exposed to an inflammatory environment induced by ISO, tumor necrosis factor alpha (TNF $\alpha$ ), and lipopolysaccharides (LPS), respectively. Our specific objectives encompass comprehending the molecular mechanisms underlying DAPA's impact on hypertrophy, fibrosis, inflammation, oxidative stress, and insulin functionality within these cellular contexts. By delving into the intricate cellular pathways influenced by DAPA, we aspire to provide mechanistic insights into its therapeutic advantages beyond glucose regulation, especially in the domains of cardiovascular and metabolic disorders.

## Results

### Reduction of cardiomyocyte hypertrophy and inflammation

#### *DAPA reduces ISO-induced cardiomyocyte hypertrophy by decreasing ROS in co-treatment and post-stimulation conditions*

Cardiomyocyte hypertrophy worsens cardiac functions and increases cardiovascular risks in patients with cardiovascular diseases. DAPA shows promise in reducing cardiovascular events in T2DM patients with pre-existing cardiovascular conditions [24–27].

To investigate the effect of DAPA on ISO-induced cardiomyocyte hypertrophy, we treated cardiomyocytes with both ISO and DAPA for 24 and 48 h, followed by an MTT assay, the colorimetric change was quantified using spectrophotometry and correlated with cell number. The ISO was administered at concentrations ranging from 2.5 to 20  $\mu$ M, with the 20  $\mu$ M concentration showing the most significant effect; thus, it was chosen to induce cardiomyocyte hypertrophy (Fig. 1A). Similarly, we conducted MTT assays for DAPA at 5, 10, and 20  $\mu$ M concentrations. Since no significant differences were observed among these concentrations, we used 10

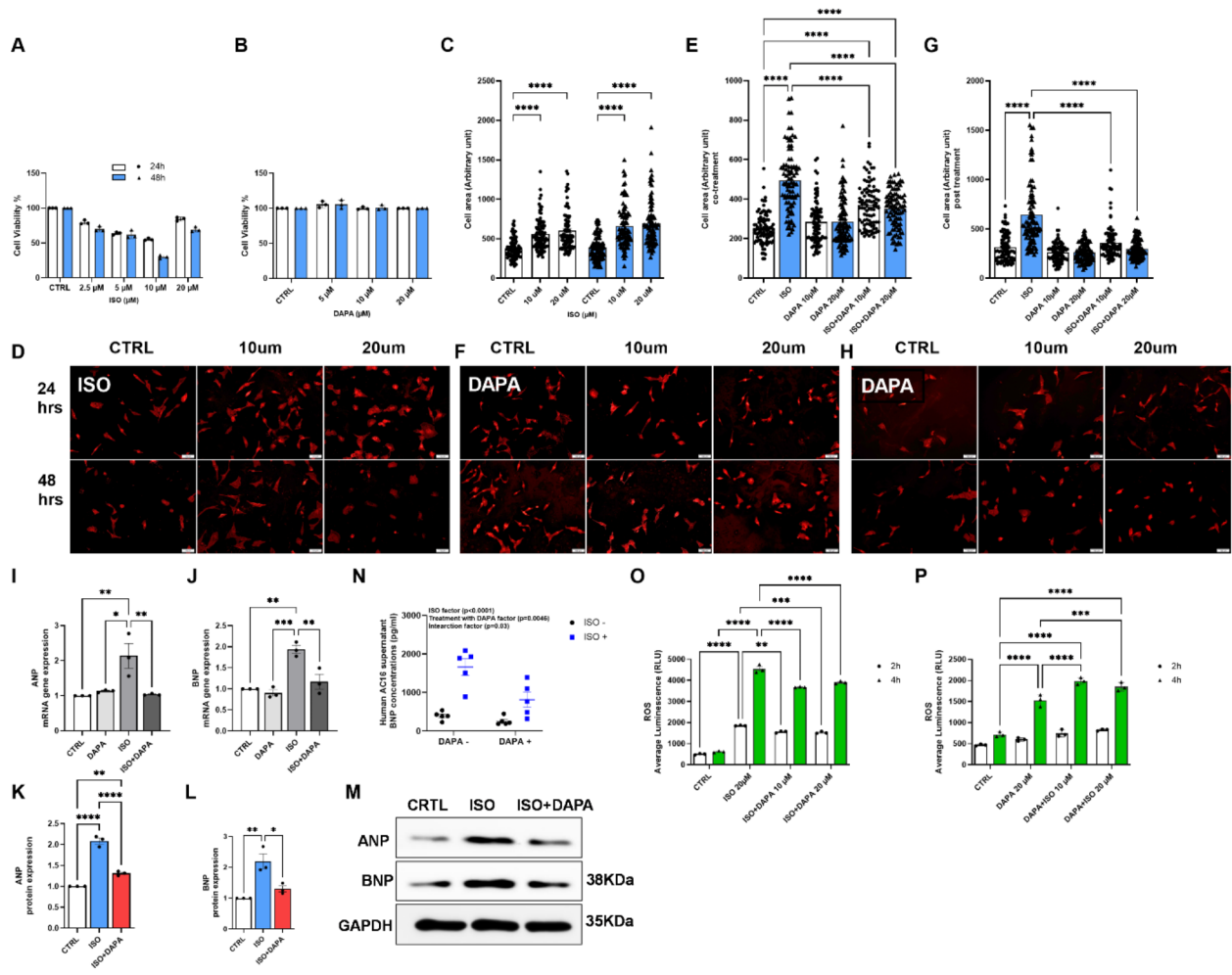


**Fig. 1** DAPA reduces ISO-induced cardiomyocyte hypertrophy by decreasing ROS in both co-treatment and post-stimulation conditions. **A** Cardiomyocytes were stimulated for hypertrophy by treating them with ISO at concentrations ranging from 2.5 to 20  $\mu\text{M}$  for 24 and 48 h, followed by cell viability assessment. **B** The impact of DAPA was investigated by treating cardiomyocytes with DAPA at concentrations ranging from 5 to 20  $\mu\text{M}$  for 24 and 48 h, followed by cell viability assessment **C** and **D** Immunofluorescence (IF) data were collected to measure cell areas of ISO-treated cardiomyocytes at ISO concentrations ranging from 10 to 20  $\mu\text{M}$  for 24 and 48 h (**D**), as well as DAPA-treated cardiomyocytes at concentrations ranging from 10 to 20  $\mu\text{M}$  for the same duration (**E** and **F**). Cell area measurements were conducted for cardiomyocytes subjected to co-treatment with ISO+DAPA for 24 h (**G** and **H**). **I-J** mRNA gene expression study for hypertrophy markers ANP and BNP, (**K**, **L**, **M**, and **N**) protein expression study and immunoblot for ANP and BNP. (**O**) ROS levels were measured in cardiomyocytes exposed to ISO stimulation for 24 h, with and without prior treatment with DAPA for the same duration. The measurements were taken at 2- and 4-hours post-stimulation. **P** The pre-protective effect of DAPA was evaluated by administering it to cardiomyocytes for 24 h before ISO stimulation, followed by ROS measurements at 2 and 4 h after ISO stimulation. In this protocol, cardiomyocytes were first stimulated with ISO for 24 h to induce hypertrophy, followed by treatment with DAPA for an additional 24 h. Immunofluorescence staining images were captured at 10x magnification, with scale bars set at 100  $\mu\text{m}$ . Error bars represent the standard error of the mean. Statistical significance is denoted as \* $p < 0.05$ , \*\* $p < 0.01$ , \*\*\* $p < 0.001$ , \*\*\*\* $p < 0.0001$

and 20  $\mu\text{M}$  concentrations to evaluate their effects on cardiomyocytes (Fig. 1B). Treatment with ISO at both 10  $\mu\text{M}$  ( $p < 0.0001$ ) and 20  $\mu\text{M}$  ( $p < 0.0001$ ) for 24 and 48 h resulted in significant hypertrophy compared to the control group (Fig. 1C and D). Moreover, co-treatment of cardiomyocytes with ISO and DAPA for 24 h significantly reduced cell hypertrophy (Fig. 1E and F). Notable differences in cell structure were observed between control and ISO-treated cells ( $p < 0.0001$ ), as well as

between ISO-treated cells and cells treated with 10  $\mu\text{M}$  ( $p < 0.0001$ ) and 20  $\mu\text{M}$  ( $p < 0.0001$ ) of DAPA. Furthermore, when cardiomyocytes were first stimulated with ISO for 24 h to induce hypertrophy and then treated with DAPA (Fig. 1G and H), we observed a highly significant ( $p < 0.0001$ ) reduction in hypertrophy in the pre-stimulated cardiomyocytes. Significant differences were noted between the control and ISO groups ( $p < 0.0001$ ), as well as between the ISO group and those treated with 10  $\mu\text{M}$

( $p < 0.0001$ ) and 20  $\mu\text{M}$  ( $p < 0.0001$ ) of DAPA. These findings indicate that DAPA protects against cardiomyocyte hypertrophy, whether administered simultaneously with ISO or after hypertrophic stimulation. In addition, we performed gene and protein expression study for the hypertrophy markers, atrial natriuretic peptide (ANP), and brain natriuretic peptide (BNP). We observed that ISO stimulation significantly increased the expression of ANP (gene expression:  $p = 0.0079$ ; protein expression:  $p < 0.0001$ , Fig. 1I and N) and BNP (gene expression:  $p = 0.0012$ ; protein expression:  $p = 0.0032$ ), compared to the control. However, co-treatment with DAPA and ISO mitigated these increases, as shown by the reduced levels of ANP (gene expression:  $p = 0.0095$ ; protein expression:  $p < 0.0001$ ) and BNP (gene expression:  $p = 0.0042$ ; protein expression:  $p = 0.0133$ , Fig. 1J and N). This highlights DAPA's role in preventing hypertrophy in ISO-induced cardiomyocytes [28, 29]. To our knowledge, various SGLT2 inhibitors have been investigated for cardiomyocyte-induced hypertrophy in humans and animal models [9, 28, 29]; however, no direct in-vitro studies have been conducted on cardiomyocytes stimulated by ISO.

Hypertrophic stimuli induce cardiomyocyte hypertrophy, often accompanied by increased ROS (Reactive oxygen species) and inflammation regulated by the AKT pathway. Activating the AKT pathway controls ROS levels and influences hypertrophy, fibrosis, and inflammation; thereby attenuating cardiac inflammation [30–36]. We examined ROS production in cardiomyocytes exposed to ISO stimulation, with or without prior treatment with DAPA. We found significant differences in ROS levels between groups treated with ISO alone and those receiving ISO+DAPA, highlighting the potential of DAPA in modulating oxidative stress and inflammation in cardiomyocytes. We investigated ROS production in cardiomyocytes exposed to ISO stimulation for 24 h, with and without prior treatment with DAPA for the same duration. ROS levels were measured at 2- and 4-hours post-stimulation. We found significant differences in ROS production between groups treated with ISO alone and those receiving ISO+DAPA at both 2 h (10  $\mu\text{M}$ :  $p = 0.0016$ , 20  $\mu\text{M}$ :  $p = 0.0006$ ) and 4 h (10  $\mu\text{M}$ :  $p < 0.0001$ , 20  $\mu\text{M}$ :  $p < 0.0001$ ) (Fig. 1O). These findings suggest that DAPA protects against cardiomyocyte dysfunction by reducing ROS levels [37]. Additionally, we explored the potential protective effect of DAPA by administering it to cardiomyocytes for 24 h before ISO stimulation. No significant differences were observed at 2 h, but a notable increase in ROS production was seen at 4 h in the DAPA pre-treated group (20  $\mu\text{M}$ :  $p < 0.0001$ ) compared to the control group. There was also a further significant increase in ROS production in the DAPA+ISO group (10  $\mu\text{M}$ :  $p < 0.0001$ , 20  $\mu\text{M}$ :  $p = 0.0009$ ) (Fig. 1P). These findings indicate complex interactions between DAPA and

ISO signaling pathways, with the timing of DAPA administration influencing ROS levels. Variations in signaling pathways and experimental conditions may also play a role. Further studies, with longer-duration DAPA treatment, may be required.

#### ***DAPA reduces ISO-induced cardiomyocytes by activating the AKT pathway, enhancing GLUT1 expression, and downregulating pro-fibrotic markers***

Studies have demonstrated the reduction of hypertrophy, fibrosis, and inflammation, along with enhanced antioxidant and mitochondrial function, through PI3K/AKT signaling activation in cardiac cells with various hypertrophy induction methods, although not with ISO specifically [10, 15]. In the current study, we assessed the gene expression directly and indirectly linked to the AKT pathway. Cardiomyocytes were treated with ISO for 6 h, followed by 24 h of DAPA treatment, and gene expression analysis was conducted. The results indicate that PI3K expression significantly increased in both the ISO+DAPA (gene expression:  $p = 0.0104$ ; protein expression  $p < 0.0001$ ) and DAPA (gene expression  $p = 0.0096$ ) groups compared to the ISO-alone group, suggesting that DAPA enhances AKT signaling (Fig. 2A). However, no differences were observed in AKT gene expression (Fig. 2B). In contrast, our protein expression study showed a significant decrease in the pAKT/AKT ratio in the ISO-treated group ( $p = 0.0011$ ) compared to control, while the addition of DAPA to ISO-treated cells significantly increased pAKT/AKT expression ( $p = 0.0001$ ) (Fig. 2K). The increase in pAKT/AKT expression when DAPA was added to ISO-treated cells suggests that DAPA enhances the phosphorylation of AKT, rather than altering its total expression. This implies that DAPA may facilitate the activation of AKT through upstream mechanisms, such as promoting PI3K activity, leading to increased phosphorylation of AKT. AKT activation is regulated through phosphorylation, therefore, DAPA's effect on increasing pAKT/AKT indicates its role in modulating this signaling pathway, potentially by enhancing the phosphorylation state of AKT, rather than through changes in total AKT expression [38]. This increase in PI3K/AKT expression is associated with reductions in fibrosis markers, such as pSMAD. The expression of pSMAD was notably elevated when treated with ISO alone compared to the control (gene expression:  $p = 0.0075$ ; protein expression:  $p = 0.0059$ ) (Fig. 2C, L and S). However, this elevated pSMAD expression was significantly reduced after adding DAPA to the ISO treatment (gene expression:  $p = 0.0342$ ; protein expression:  $p = 0.0433$ ). These findings suggest that DAPA not only enhances PI3K/AKT signaling but also mitigates the pro-fibrotic effects induced by ISO. No significant differences were observed in  $\alpha\text{SMA}$  gene expression in the



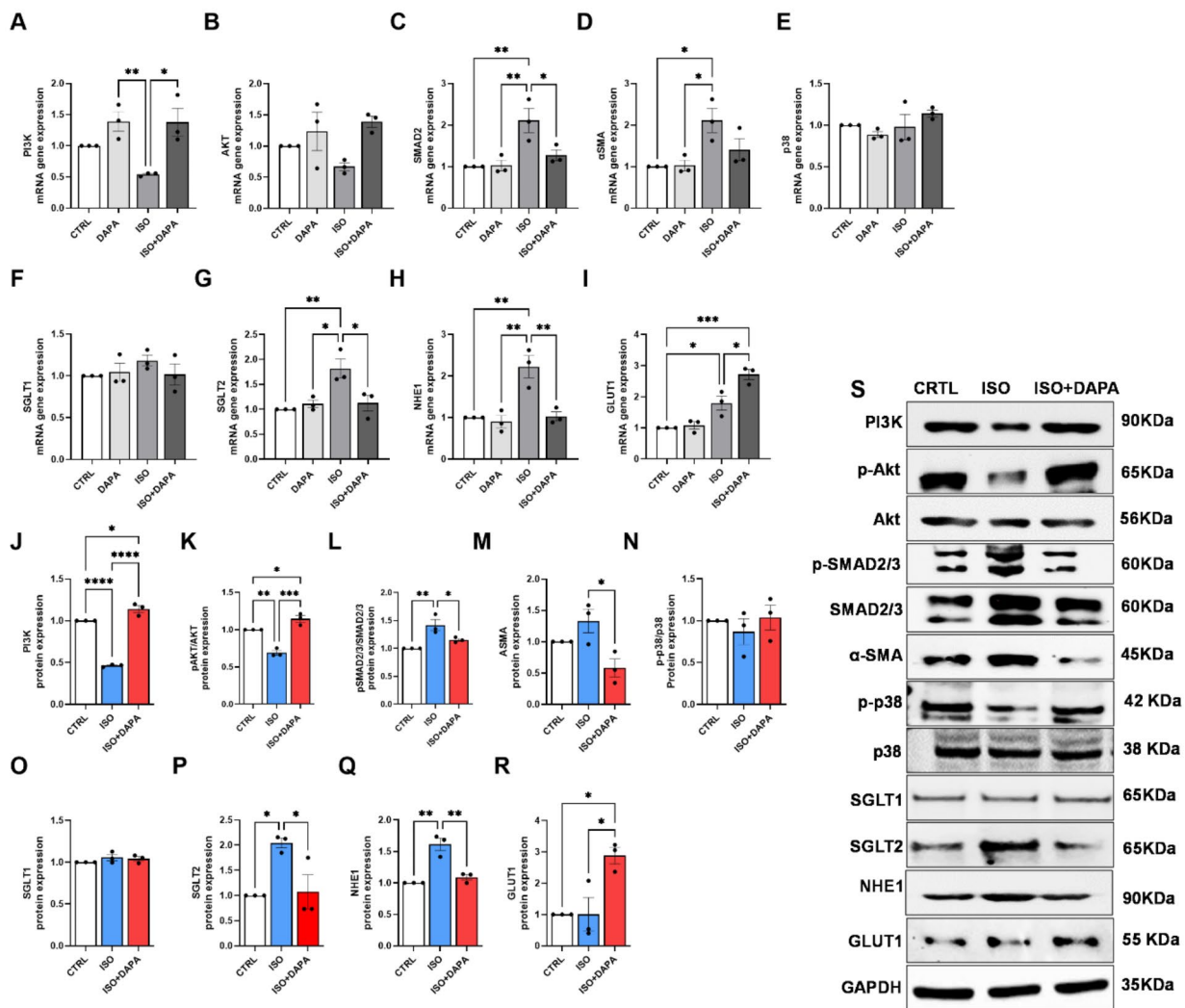


**Fig. 2** DAPA reduces ISO-induced cardiomyocytes by Activating the AKT Pathway, enhancing GLUT1 expression, and downregulating pro-fibrotic markers. **A-I** qPCR and **J-R** Western blot analyses were performed to assess the gene and protein expression levels of PI3K/AKT, fibrosis markers (pSMAD2, ASMA), the apoptosis marker (P-p38), sodium-glucose cotransporters (SGLT-1 and SGLT-2), the sodium-hydrogen exchanger (NHE-1), and the glucose transporter protein (GLUT-1). **S** Representative Western blot images for the proteins. Statistical significance is represented as \* $p < 0.05$ , \*\* $p < 0.01$ , \*\*\* $p < 0.001$ , and \*\*\*\* $p < 0.0001$

ISO+DAPA-treated group. Interestingly, there was a significant reduction at the protein level (Fig. 2D, M, and S). The discrepancy between the unchanged gene expression and the significant decrease in  $\alpha$ SMA protein expression ( $p = 0.0198$ ) could be attributed to post-transcriptional or post-translational modifications. DAPA could exert effects that stabilize or degrade the  $\alpha$ SMA protein independently of gene transcription, which is not uncommon in signaling pathways where protein regulation can occur at multiple levels. Furthermore, we screened for the apoptotic marker p38, and no significant differences were observed between the studied groups in both gene and protein expression analyses (Fig. 2E, N, and S), suggesting that the observed effects of DAPA are not attributable

to changes in apoptosis. This further supports the notion that DAPA's action is more focused on modulating fibrosis and hypertrophy rather than apoptosis.

SGLT2 inhibitors, like DAPA, influence cellular ion balance by reducing sodium reabsorption in the kidneys, which can impact NHE1 activity. This interaction is crucial for their cardioprotective effects, including improvements in glucose metabolism, reduced inflammation, and reduced oxidative stress within cardiovascular cells [39–41]. To delve deeper, we further assessed the gene expression of SGLT2, NHE1, and GLUT1 in ISO-induced cardiomyocytes. We observed an increase in SGLT2 expression following ISO stimulation (Fig. 2G, P, and S) compared to the control (gene expression:

$p=0.0095$ ; protein expression  $p=0.0256$ ). However, the addition of DAPA to the ISO-treated cardiomyocyte significantly reduced SGLT2 expression in the ISO+DAPA group (gene expression:  $p=0.0237$ ; protein expression  $p=0.0347$ ). This reduction could be due to DAPA's ability to restore inflamed cardiac cells, influencing the pathway's responsiveness to inhibitors, particularly the NHE1 pathway. NHE1 regulates intracellular pH and cell volume by exchanging intracellular hydrogen ions for extracellular sodium ions. This pathway is crucial in ROS production and inflammatory responses within cardiovascular cells. By modulating NHE1 activity, DAPA helps reduce oxidative stress and inflammation, providing long-term cardioprotective effects [42–44]. Our results indicated that DAPA exerts its effects by influencing the activity of key signaling molecules involved in oxidative stress and inflammation. The significant induction of NHE1 expression (Fig. 2H, Q, and S) upon ISO stimulation (gene expression:  $p=0.0031$ ; protein expression:  $p=0.0012$ ) was attenuated with the addition of DAPA (gene expression:  $p=0.0035$ ; protein expression:  $p=0.0027$ ), suggesting that DAPA helps to stabilize NHE1 activity, thereby reducing ROS production and inflammation over time. Further, the activity of NHE1 can be influenced by changes in cellular sodium levels resulting from SGLT2 inhibition, which may impact intracellular pH and calcium regulation. We observed a significant increase in GLUT1 expression in the ISO+DAPA ( $p=0.0118$ ) compared to the ISO-alone group. Additionally, there was an increase in GLUT1 expression in the ISO-treated group ( $p=0.0002$ ) compared to the control group (Fig. 2I, R and S). The increase in GLUT1 expression with ISO+DAPA treatment suggests a cellular adaptation to maintain glucose homeostasis despite the reduced glucose reabsorption due to SGLT2 inhibition. This enhanced glucose uptake could potentially modulate cellular metabolism and contribute to the observed DAPA's effects on NHE1 activity. The interplay between these transporters and metabolic pathways highlights the complex mechanisms by which DAPA exerts its effects, potentially offering new insights into its therapeutic benefits and the regulation of intracellular pH and calcium levels [45]. Furthermore, we analyzed the expression of SGLT1 but did not find any significant differences between the treated groups (Fig. 2F, O, and S). One possible reason for this could be that the effects of DAPA, a selective SGLT2 inhibitor, are primarily exerted through SGLT2 rather than SGLT1. While SGLT1 is also involved in glucose transport, its expression and role may not be as strongly influenced by DAPA in this context. Additionally, the expression of SGLT1 might be regulated by different mechanisms that are not directly affected by the PI3K/AKT or hypertrophy-related signaling pathways. Therefore, the lack of significant changes in SGLT1 expression suggests that

DAPA's cardioprotective effects might be more related to its impact on SGLT2 or other signaling cascades, rather than on SGLT1 specifically [46].

#### **DAPA inhibits ISO-induced cardiomyocyte inflammation and modulates antioxidant responses**

Inflammation and oxidative stress play important roles in cardiomyocyte dysfunction. We investigated the effects of DAPA on inflammation and antioxidant expression. Our results showed that NLRP3 expression increased following ISO induction but was significantly reduced after DAPA treatment (gene expression:  $p=0.0032$ ; protein expression:  $p=0.007$ ) (Fig. 3A, F, and K), indicating that DAPA exerts a potent anti-inflammatory effect. Moreover, the marked upregulation of NLRP3 in the ISO-alone group was accompanied by an increase in NRF2 (Nuclear factor erythroid 2-related factor 2) expression in the DAPA-treated group (Fig. 3B). Given that the AKT/PI3K pathway is crucial for NRF2 activation [45], our results demonstrate that NRF2 expression significantly increased following DAPA stimulation (Fig. 3B, G, and K). However, this increase was mitigated when ISO was introduced (gene expression:  $p=0.025$ ; protein expression:  $p<0.0001$ ). Importantly, the reduction in NRF2 expression caused by ISO was effectively restored with the addition of DAPA to the ISO-treated group (gene expression:  $p<0.0001$ ; protein expression:  $p<0.0001$ ). These findings suggest that DAPA has anti-inflammatory properties and enhances the antioxidant response by promoting NRF2 activation, thereby countering the detrimental effects of ISO-induced stress. We further measured the expression of antioxidant and cytoprotective genes such as NQO1 (NAD(P)H Quinone Dehydrogenase 1) and HO-1 (Heme Oxygenase 1). NQO1 gene expression was reduced in the ISO-treated group ( $p=0.0116$ ), but no significant differences were observed in the protein expression study (Fig. 3C, H, and K). This discrepancy may be due to the post-transcriptional regulation of NQO1, where factors such as mRNA stability or translational efficiency could influence protein levels without affecting mRNA expression directly. In contrast, HO-1 expression was significantly elevated in the DAPA+ISO treated group (gene expression:  $p=0.0425$ ; protein expression:  $p=0.0032$ ) (Fig. 3D, I, and K). The impaired expression of these antioxidant and cytoprotective genes in the ISO-treated group suggests that ISO induces oxidative stress and disrupts cellular defense mechanisms. DAPA appears to counteract these effects by enhancing NRF2 activation, which in turn upregulates the expression of NQO1 and HO-1. This restoration of gene expression indicates that DAPA not only mitigates the oxidative damage caused by ISO but also supports cellular resilience by promoting the synthesis of key antioxidant and cytoprotective genes.

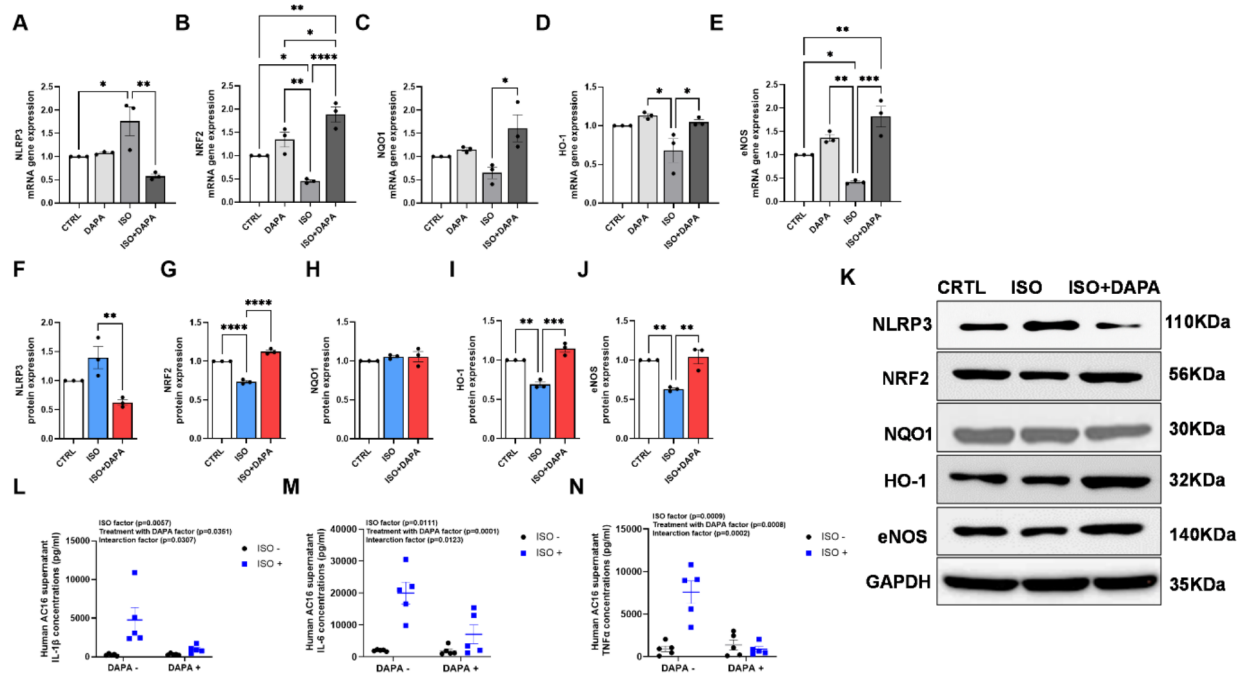


**Fig. 3** DAPA inhibits ISO-induced cardiomyocyte inflammation and modulates antioxidant responses. **A-E** qPCR and **F-J** Western blot analyses were performed to evaluate the gene and protein expression levels of inflammatory markers (NLRP3), antioxidant markers (NRF2, NQO1, and HO-1), and endothelial nitric oxide synthase (eNOS). **K** Representative Western blot images for these proteins are presented. **K-N** ELISA assays were conducted to measure IL-1 $\beta$ , IL-6, and TNF $\alpha$  levels in the cell supernatant. Statistical significance is indicated as \* $p < 0.05$ , \*\* $p < 0.01$ , \*\*\* $p < 0.001$ , and \*\*\*\* $p < 0.0001$

We also examined the expression of endothelial nitric oxide synthase (eNOS) in cells treated with ISO and ISO+DAPA. As shown in our gene and protein expression analyses (Fig. 3E, J, and K), eNOS expression significantly decreased following ISO treatment (gene expression:  $p = 0.0020$ ; protein expression:  $p = 0.0055$ ) and reversed when DAPA was added to the ISO treatment (gene expression:  $p = 0.0001$ ; protein expression:  $p = 0.0032$ ). The decrease in eNOS expression due to ISO may stem from the oxidative stress and inflammatory response ISO induces, negatively affecting eNOS expression and function. ISO is known to cause endothelial dysfunction by reducing nitric oxide availability, essential for vascular health and function. The restoration of eNOS expression with DAPA suggests that DAPA may activate signaling pathways that enhance eNOS expression, possibly via the PI3K/AKT pathway, which is known to positively regulate eNOS [47, 48]. Therefore, DAPA appears to counteract ISO's negative effects and supports endothelial function by maintaining eNOS expression and activity.

Additionally, we assessed the secretion levels of key pro-inflammatory markers, analyzing the expression of inflammatory cytokines IL-1 $\beta$  (Interleukin 1 beta), IL-6 (Interleukin), and TNF $\alpha$ , which are crucial in both physiological and pathological processes [49]. For IL-1 $\beta$ ,

there were significant effects from ISO and DAPA treatment, with a significant interaction between the two ( $p < 0.05$ ), suggesting that DAPA's effect on IL-1 $\beta$  expression depends on the presence of ISO (Fig. 3L). Similarly, IL-6 secretion level was significantly affected by ISO and DAPA, with a significant interaction ( $p < 0.05$ ), indicating that DAPA's impact on IL-6 expression is also condition-dependent (Fig. 3M). For TNF $\alpha$ , we observed significant effects from both ISO and DAPA with a notable interaction between the two ( $p < 0.05$ ), suggesting that DAPA's influence on TNF $\alpha$  expression varies based on ISO treatment (Fig. 3N). These results highlight the important roles of both ISO and DAPA in modulating IL-1 $\beta$ , IL-6, and TNF $\alpha$  levels, with significant interactions warrant further investigation. Understanding the regulation of these inflammatory cytokines is essential for exploring their role in disease progression and treatment responses, particularly regarding DAPA effects on inflammation and metabolic health [50].

**DAPA effects on human aortic endothelial cells**

**DAPA reduces TNF $\alpha$ -induced inflammation in AECs via modulating the AKT pathway**

Given the limited data and the lack of molecular studies, we investigated the role of DAPA on AECs, particularly to identify any similarities in pathways affected by DAPA



in both AECs and ISO-stimulated cardiomyocytes. To determine the optimal concentration of DAPA for treating AECs we conducted an MTT assay with various treatments: TNF $\alpha$  alone (Fig. 4A), DAPA alone (Fig. 4B), pre-treatment with TNF $\alpha$  for 24 h followed by DAPA (Fig. 4C), and co-treatment with TNF $\alpha$ +DAPA for 24 h (Fig. 4D). The optimal concentrations were identified as 100 ng/ml for TNF $\alpha$  (determined by EC50) and 1  $\mu$ M for DAPA, which were used in all subsequent experiments.

Gene expression analysis demonstrated that DAPA treatment significantly upregulated AKT expression ( $p=0.043$  vs. control, Fig. 4E). However, AKT expression was significantly reduced following TNF $\alpha$  induction (gene expression:  $p=0.0008$ ; protein expression:  $p<0.0001$ ) (Fig. 4E, V, and Z). Notably, when DAPA was introduced to TNF $\alpha$ -stimulated cells, AKT and pAKT expression increased significantly (gene expression:  $p=0.0034$ ; protein expression:  $p<0.0001$  for TNF $\alpha$  alone vs. TNF $\alpha$ +DAPA). The AKT pathway significant role in

cell survival and metabolism suggests that DAPA helps counteract TNF $\alpha$ -induced stress by promoting AKT activity. The ability of DAPA to restore AKT expression in the presence of TNF $\alpha$  indicates its potential protective effect against inflammation-induced cellular stress, highlighting its therapeutic potential in conditions characterized by inflammatory stress and impaired AKT signaling [51, 52]. Similarly, PI3K expression was increased in the DAPA-treated group compared to controls ( $p=0.002$ ), but this increase was significantly reversed after treatment with TNF $\alpha$  ( $p<0.0001$ ) (Fig. 4F). However, when cells were co-treated with DAPA+TNF $\alpha$ , the inhibition of PI3K was reversed, with PI3K expression significantly increasing again ( $p<0.001$  for TNF $\alpha$ -alone vs. DAPA+TNF $\alpha$  groups). The PI3K/AKT pathway is essential for promoting cell growth and survival, and the activation of PI3K leads to the production of PIP3 (Phosphatidylinositol (3,4,5)-trisphosphate (PtdIns(3,4,5) P3), which recruits and activates AKT, thereby promoting

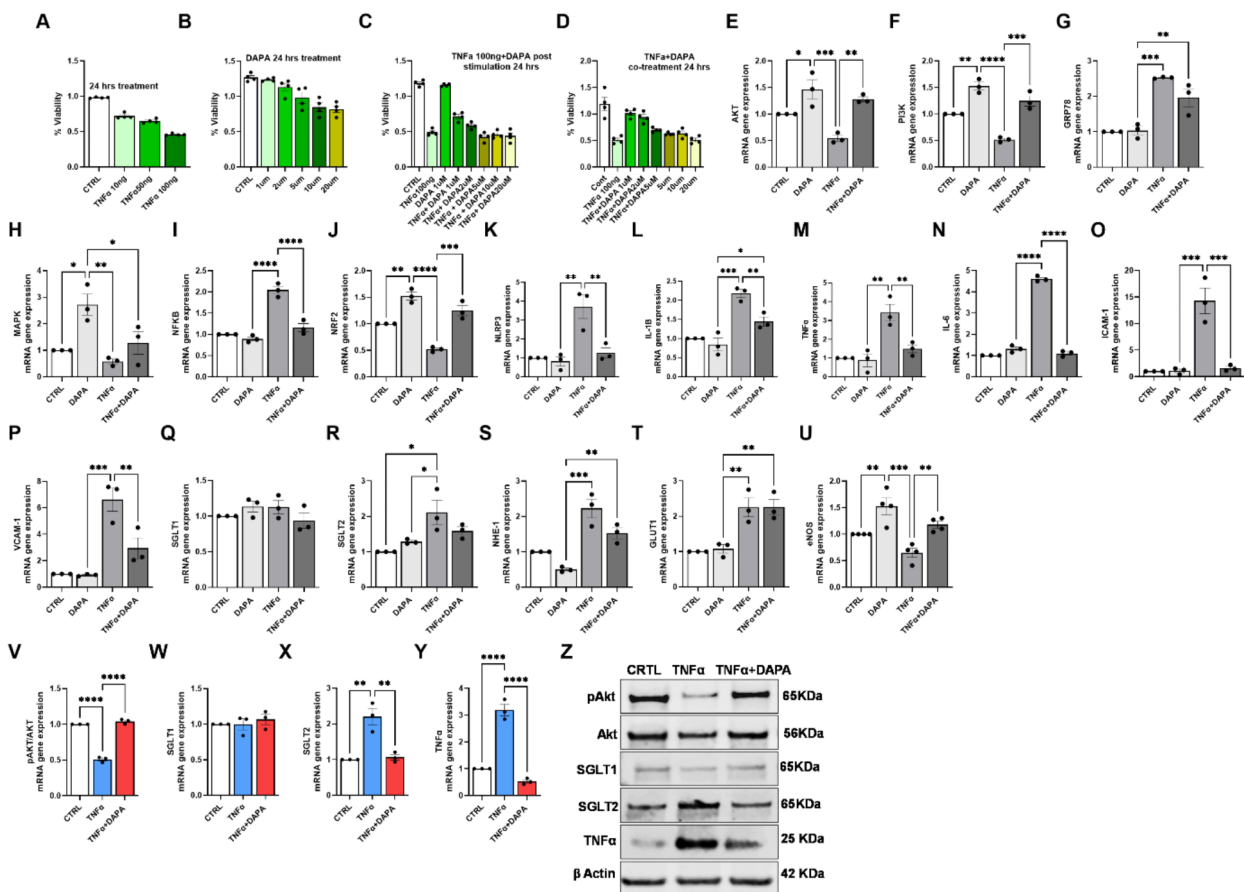


**Fig. 4** DAPA reduces TNF $\alpha$ -induced inflammation in AECs by modulating the AKT pathway. **A-D** MTT assays were performed with various treatments: **A** TNF $\alpha$  alone, **B** DAPA alone, **C** pre-treatment with TNF $\alpha$  for 24 h followed by DAPA, and **D** co-treatment with TNF $\alpha$  + DAPA for 24 h. **E-U** mRNA gene expression studies for AKT, PI3K, mitochondrial marker (GRP78), inflammation and antioxidant markers (MAPK, NF- $\kappa$ B, NRF2, NLRP3, IL-1 $\beta$ , TNF $\alpha$ , IL-6), adhesion molecules (ICAM, VCAM), SGLT1, SGLT2, NHE-1, GLUT-1 and eNOS. **V-Y** protein expression study for pAKT/AKT, SGLT1, SGLT2 and TNF $\alpha$  and **Z** Representative Western blot images for the proteins. Statistical significance is indicated as \* $p<0.05$ , \*\* $p<0.01$ , \*\*\* $p<0.001$ , \*\*\*\* $p<0.0001$

survival and growth signals. The ability of DAPA to upregulate PI3K expression even in the presence of TNF $\alpha$  suggests that DAPA enhances the cell's capacity to resist inflammatory damage and promotes repair mechanisms [53, 54]. Furthermore, we study how TNF $\alpha$  affects GRP78 (Glucose-regulated protein). GRP78 is an endoplasmic reticulum (ER) stress marker, and its expression is linked to the protective effects observed in the PI3K/AKT signaling pathways. We observed an increase in GRP78 expression in the TNF $\alpha$ -alone group compared to the DAPA group ( $p=0.0003$ ) (Fig. 4G). Additionally, there was a reduction in GRP78 expression in the co-treated TNF $\alpha$ +DAPA group versus the TNF $\alpha$ -alone group; and despite being not statistically significant ( $p>0.05$ ), a net reduction was noted. The reduction in GRP78 with DAPA treatment suggests that DAPA might alleviate the ER stress induced by TNF $\alpha$ , further supporting its protective effect on AECs. This reduction in ER stress could also contribute to the overall cellular resilience against inflammatory damage, enhancing cell survival and function by upregulating critical signaling pathways such as AKT and PI3K. The MAPK pathway is involved in cellular responses to a variety of stress signals, and its activation is associated with inflammation, apoptosis, and cell differentiation [55]. DAPA's ability to modulate this pathway suggests it might influence AECs' responses to inflammatory stress by affecting MAPK expression [56]. Our results showed that DAPA treatment increased MAPK expression compared to the control ( $p=0.015$ , Fig. 4H). In contrast, MAPK expression was significantly reduced in the TNF $\alpha$  group ( $p=0.0041$ ). Interestingly, when DAPA was added to TNF $\alpha$ -stimulated cells, MAPK expression was elevated, although the increase was not statistically significant in the TNF $\alpha$ +DAPA group. This suggests that DAPA may at least partially restore MAPK levels, potentially influencing inflammatory signaling pathways. These results highlight the complex interplay between DAPA and TNF $\alpha$  and emphasize the need for further studies to elucidate how DAPA modulates MAPK and related inflammatory pathways in AECs. Based on our observations of inflammatory pathway activation and inhibition in AECs, we extended our study to examine a broader set of inflammatory genes involved in regulatory processes. Cells stimulated with TNF $\alpha$  alone showed a significant upregulation of inflammatory genes, including NF- $\kappa$ B-nuclear factor kappa B ( $p<0.0001$ , Fig. 4I), NLRP3-NLR family pyrin domain containing 3 ( $p=0.0058$ , Fig. 4K), IL-1 $\beta$  ( $p=0.0091$ , Fig. 4M), TNF $\alpha$  (gene expression  $p=0.0088$ ; protein expression  $p<0.0001$ , Fig. 4M, Y, Z), and IL-6 ( $p<0.0001$ , Fig. 4N). This marked increase underscores the strong pro-inflammatory effects of TNF $\alpha$ . However, treatment with DAPA suppressed this rise in the TNF $\alpha$ +DAPA group, as evidenced by decreased expression of NF- $\kappa$ B ( $p<0.0001$ , Fig. 4I),

NLRP3 ( $p=0.0020$ , Fig. 4J), IL-1 $\beta$  ( $p=0.0002$ , Fig. 4M), TNF $\alpha$  (gene expression  $p=0.0016$ ; protein expression  $p<0.0001$ , Fig. 4M, Y, Z), and IL-6 ( $p<0.0001$ , Fig. 4N), demonstrating its potent anti-inflammatory effects that counteract the pro-inflammatory actions of TNF $\alpha$ . Additionally, we investigated NRF2, an antioxidant gene, which showed increased expression with DAPA compared to the control group ( $p=0.0016$ ) (Fig. 4J). NRF2 expression ( $p<0.0001$  for TNF $\alpha$ -alone group vs. DAPA group) was reduced in TNF $\alpha$  but this reduction was reversed with the addition of DAPA ( $p=0.0002$ ), suggesting the DAPA's role in mitigating oxidative stress through the NRF2 pathway. NRF2 regulates the expression of antioxidant proteins crucial for protecting against oxidative damage triggered by inflammation and injury. The elevation in NRF2 expression with DAPA suggests that DAPA enhances the cell's antioxidant defenses, further emphasizing its potential therapeutic benefit in combating inflammation-associated oxidative stress [57, 58].

The adhesion molecules like ICAM-1 (Intercellular Adhesion Molecule 1) and VCAM-1 (Vascular cell adhesion molecule 1) are crucial in inflammation and atherosclerosis, owing to their involvement in the process of leukocyte recruitment to the sites of inflammation. Here the expression of ICAM-1 (Fig. 4O) and VCAM-1 (Fig. 4P) was increased in the TNF $\alpha$ -alone group vs. DAPA group (ICAM  $p=0.0003$ , VCAM  $p=0.0006$ ) and was reduced in the co-treated TNF $\alpha$ +DAPA group vs. TNF $\alpha$ -alone group (ICAM  $p=0.0004$ , VCAM  $p=0.0097$ ). Their reduction with DAPA treatment indicates the DAPA potential to reduce vascular inflammation via its inhibitory effect on endothelial activation and leukocyte adhesion, which are critical steps in the atherosclerotic process [59, 60].

We next investigated the expression of SGLT2, sodium/hydrogen exchanger 1 (NHE1), and glucose transporter 1 (GLUT1), given their crucial roles in the relationship between inflammation and oxidative stress, especially in the context of DAPA's function as an SGLT2 inhibitor. In the TNF $\alpha$ -alone group, there was a significant increase in SGLT2 expression (gene expression:  $p=0.0481$ ; protein expression:  $p=0.0024$  vs. control, Fig. 4R, X, and Z) and its upstream regulator NHE-1 ( $p=0.0002$  vs. DAPA group, Fig. 4S). Interestingly, while we observed a decrease in protein expression in TNF $\alpha$ +DAPA co-treated group compared to TNF $\alpha$  alone (protein expression:  $p=0.0032$  vs. TNF $\alpha$ , Fig. 4R, X, and X) but this was not reflected in gene expression levels, suggesting that DAPA may influence post-transcriptional regulatory mechanisms that affect protein stability or translation without significantly altering gene transcription. Further investigation is needed in a greater sample size. The reduction in SGLT2 and NHE-1 expression suggests that DAPA may limit glucose uptake in endothelial cells,

potentially lowering glucose-induced oxidative stress [61, 62]. Further, we observed GLUT1 expression (Fig. 4T) significantly increased in both the TNF $\alpha$ -alone group ( $p=0.0086$  vs. DAPA group) and the TNF $\alpha$ +DAPA co-treatment group ( $p=0.0083$  vs. DAPA group). GLUT1 is crucial for basal glucose uptake and likely maintains its expression to ensure a steady supply of essential glucose during stress conditions. The lack of GLUT1 expression difference between the DAPA+TNF $\alpha$  co-treatment group compared to the TNF $\alpha$ -alone group implies that while DAPA may impact multiple pathways, it might not influence GLUT1 expression under conditions of TNF $\alpha$ -induced stress nor substantially alter the expression of glucose transporters in the presence of TNF $\alpha$  [63]. Additionally, we also studied the gene expression analysis for SGLT1, and no significant differences were observed between the study groups (Fig. 4Q, W, and Z), aligning with the protein expression results.

Additionally, we study the expression of eNOS (endothelial nitric oxide) which is a pivotal regulator of vascular homeostasis. We found an increase in eNOS expression in the control and DAPA-treated groups (gene expression:  $p=0.045$ ) (Fig. 3U). Following TNF $\alpha$  administration, eNOS expression was significantly decreased ( $p=0.0001$ ) and then restored when treated with DAPA ( $p=0.0086$ ). This suggests that DAPA exerts protective effects by enhancing eNOS expression, thereby facilitating vasodilation and preserving vascular function amid inflammatory conditions. The restoration and elevation of eNOS expression by DAPA underscore its potential to counteract the detrimental effects of inflammation on endothelial function [30, 64]. Overall, DAPA demonstrated a protective role in AECs against TNF $\alpha$ -induced stress by modulating key signaling pathways, including AKT/PI3K, MAPK (Mitogen-activated protein kinases), and inflammatory pathways. The regulation of adhesion molecules and SGLT2 further supports its potential therapeutic benefits in vascular health.

#### **DAPA effects on extracellular matrix (ECM) remodeling, vascular function, and inflammation in AECs**

To validate the observed changes in SGLT2 expression, we conducted immunofluorescence (IF) analysis (Fig. 5A and B). Consistent with our earlier findings, our results revealed a significant increase in SGLT2 expression in the TNF $\alpha$ -induced group compared to the control (Fig. 5A,  $p<0.0001$ ). The increased expression due to TNF $\alpha$  induction was significantly reduced after adding DAPA to the TNF $\alpha$ -stimulated group ( $p=0.0441$ , Fig. 5A and B).

Further, IF investigation into ICAM expression (Fig. 5C, D, and G) revealed a marked increase in ICAM expression in the TNF $\alpha$ -induction group compared to the control group ( $p<0.0001$ ). Notably, this upregulation was reversed in the DAPA+TNF $\alpha$  co-treatment group

compared to the TNF $\alpha$ -alone induction group ( $p=0.04$ ). To understand deeper, we determined the ICAM-1 and VCAM-1 secretion levels. ICAM-1 and VCAM-1 secretion show a significant interaction between the DAPA+TNF $\alpha$  co-treatment group ( $p<0.05$ , Fig. 5G and H). This observed decrease in ICAM and VCAM expression following co-treatment with DAPA suggests its potential to mitigate TNF $\alpha$ -induced endothelial cell activation and inflammation.

Next, we assessed collagen expression (Fig. 5E and F) to probe the potential alterations in extracellular matrix (ECM) remodeling. Significantly higher collagen deposition was observed in the TNF $\alpha$ -induction group compared to the control group ( $p<0.0001$ ), indicating TNF $\alpha$ -induced perturbations in ECM dynamics. These alterations may contribute to the observed vascular remodeling and inflammation in endothelial cells subjected to TNF $\alpha$  stimulation. The increased collagen deposition reflects an aberrant extracellular matrix turnover, indicative of tissue remodeling associated with inflammatory processes [65, 66]. However, despite DAPA's potential to mitigate inflammation, no reduction in collagen deposition was observed in the TNF $\alpha$ +DAPA co-treatment group in comparison to the TNF $\alpha$ -alone group ( $p>0.05$ , Fig. 5E and F). This suggests that while DAPA may have anti-inflammatory effects, it may not directly influence collagen synthesis or deposition under these experimental conditions.

Additionally, we measured the levels of eNOS, iNOS (Inducible nitric oxide synthase), and NO (Nitric oxide) a key indicators of endothelial function. NO is essential for maintaining vascular homeostasis, regulating blood flow, and inhibiting inflammation. The balance between eNOS, which facilitates the beneficial production of NO, and iNOS, which is often associated with inflammatory responses, is critical for preserving endothelial health [67]. For eNOS, we observed effects from ISO and DAPA treatment, with a significant interaction between the two ( $p<0.05$ ), suggesting a synergistic effect on enhancing NO bioavailability and promoting endothelial function (Fig. 5I). Similarly, iNOS levels were influenced by ISO and DAPA, with a significant interaction ( $p<0.05$ ), indicating their combined effect in reducing inflammation-related NO production (Fig. 5J). Furthermore, for NO, significant effects were observed from both ISO and DAPA, with a notable interaction between the two ( $p<0.05$ ), suggesting their role in modulating NO levels to enhance vascular health and counteract inflammation (Fig. 5K). These findings underscore the pivotal roles of both ISO and DAPA in modulating endothelial cell function and inflammatory responses.

We also analyzed the expression of inflammatory cytokines IL-1 $\beta$ , IL-6, and TNF $\alpha$ , as these are critical markers of inflammation and endothelial cell activation.



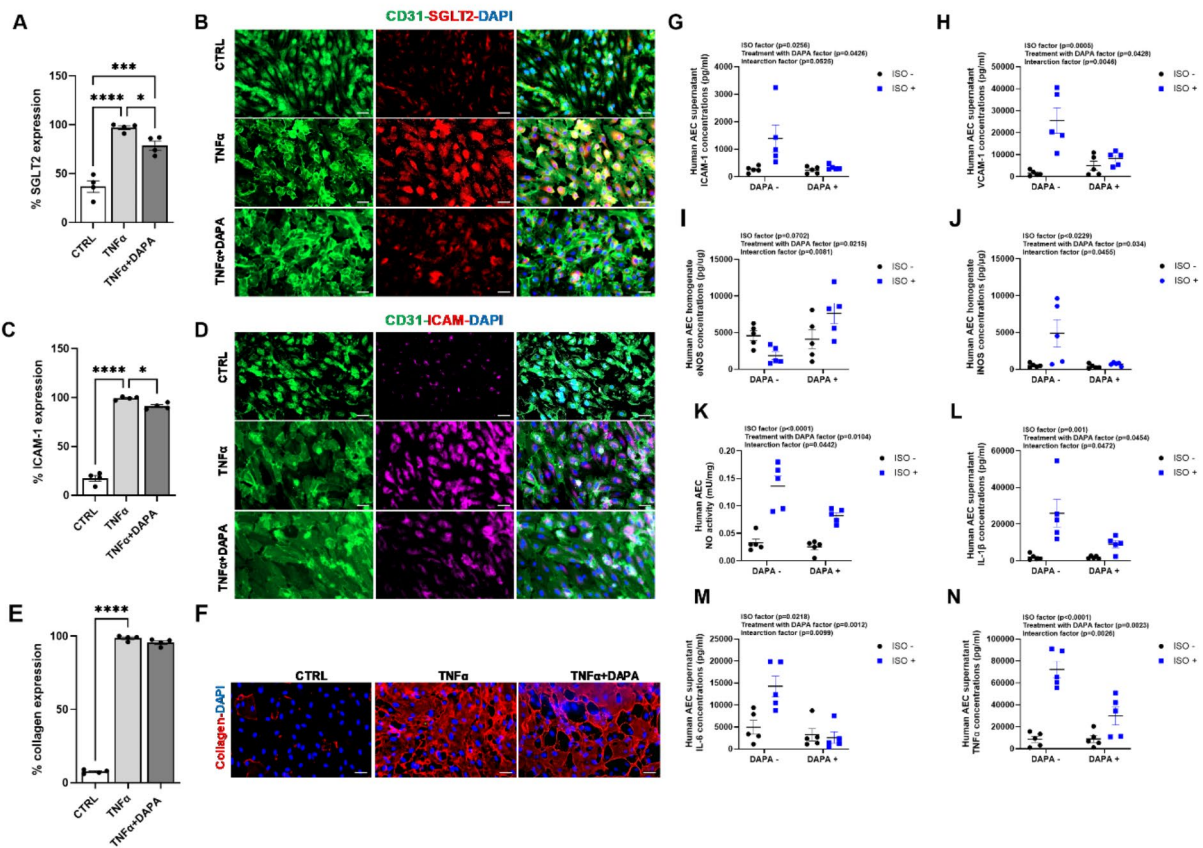


**Fig. 5** DAPA effects on extracellular matrix (ECM) remodeling, vascular function, and inflammation in AECs. **A-B** Cell counting and representative images of immunofluorescence staining for SGLT2 **C-D** ICAM and **E-F** collagen expression. **G-N** ELISA measurement of ICAM-1, VCAM-1, eNOS, iNOS, NO, IL-1 $\beta$ , IL-6 and TNF $\alpha$ . Immunofluorescence staining images were captured at 20x magnification, with scale bars set at 100  $\mu$ m. Statistical significance is denoted as \* $p < 0.05$ , \*\* $p < 0.01$ , \*\*\* $p < 0.001$ , \*\*\*\* $p < 0.0001$

IL-1 $\beta$  is a potent pro-inflammatory cytokine that plays a central role in initiating and perpetuating inflammatory responses. Significant effects on IL-1 $\beta$  expression were observed from ISO treatment and DAPA administration, with a significant interaction between the two ( $p < 0.05$ ), indicating a combined effect in reducing IL-1 $\beta$  levels (Fig. 5L). IL-6, another key pro-inflammatory cytokine involved in chronic inflammation and endothelial dysfunction, was significantly influenced by ISO and DAPA, with a notable interaction ( $p < 0.05$ ), suggesting their cooperative action in modulating IL-6 secretion (Fig. 5M). TNF $\alpha$ , which is a master regulator of inflammation and can trigger endothelial dysfunction [68] by promoting the expression of adhesion molecules and other inflammatory mediators, we found significant effects from both ISO and DAPA, with a notable interaction between the two ( $p < 0.05$ ), suggesting that the combination of ISO and DAPA exerts a strong regulatory effect on TNF $\alpha$  levels (Fig. 5N). These results highlight the important roles of both ISO and DAPA in modulating the levels of key inflammatory cytokines, including IL-1 $\beta$ ,

IL-6, and TNF $\alpha$ , thereby influencing inflammation, endothelial cell activation, and overall vascular health.

### DAPA effects on SC- $\beta$ cells

#### DAPA improves insulin functionality of SC- $\beta$ cells

The role of DAPA in managing T2DM is well-documented [27, 69, 70]. DAPA's actions intersect with pathways relevant to both diabetes and cardiovascular health. By inhibiting SGLT2, DAPA improves glucose regulation, reduces inflammation, and enhances vascular function, thereby offering benefits for both diabetes and cardiovascular diseases [71, 72]. It has been shown by the current experiments that DAPA counteracts cardiomyocyte hypertrophy by activating the AKT pathway, reducing inflammation, and promoting antioxidant activity. While DAPA is primarily used as a diabetes medication, it raises the question of whether its action on diabetes involves the same pathways or operates through separate mechanisms. Studies have not conclusively determined whether DAPA acts directly on  $\beta$ -cells or islets, or how DAPA



influences aspects such as cell identity, trans-differentiation, and other cellular processes.

To address this knowledge gap, we conducted in-vitro experiments to investigate the action of DAPA on SC-β cells generated via a well-established six-step protocol [73] (Fig. 6A and B) and confirmed their responsiveness to glucose-stimulated insulin secretion (GSIS) assay (Fig. 6E). Their cellular identity was verified via co-staining for NKX6.1(NK6 Homeobox 1) and insulin using immunofluorescence (Fig. 6C, Suppl. Figure 3E) and flow cytometry (Fig. 6D, Suppl. Figure 3 A). To evaluate the effects of DAPA on the insulin functionality of SC-β cells, we exposed these cells to varying concentrations of DAPA, ranging from 0.25 to 10 μM, for 24 h using a concentration of 0.5 μM for subsequent analyses, we observed no significant difference ( $p > 0.05$ ) between the DAPA-treated cells and control group (Fig. 6G, Suppl. Figure 3B-D). However, an intriguing enhancement in

insulin functionality was noted in the DAPA-treated group compared to the control ( $p = 0.0245$ , Fig. 6H) indicating that DAPA improved the functionality of SC-β cells without altering their cell identity. Additionally, we performed a glucose-stimulated insulin secretion (GSIS) assay in human islets to study the impact of DAPA. Our results show no significant differences in the overall insulin secretion response following DAPA treatment compared to the control group (Fig. 6I). Further experiments are needed with a larger sample size to confirm these findings and to explore potential effects in greater detail.

**DAPA modulates SC-β cell function, inflammation, and stress response**

Studies have shown that SGLT2 inhibitors, like DAPA, are associated with promoting islet cell proliferation and trans-differentiation [20, 74, 75]. Consequently, we focused on examining how DAPA treatment might

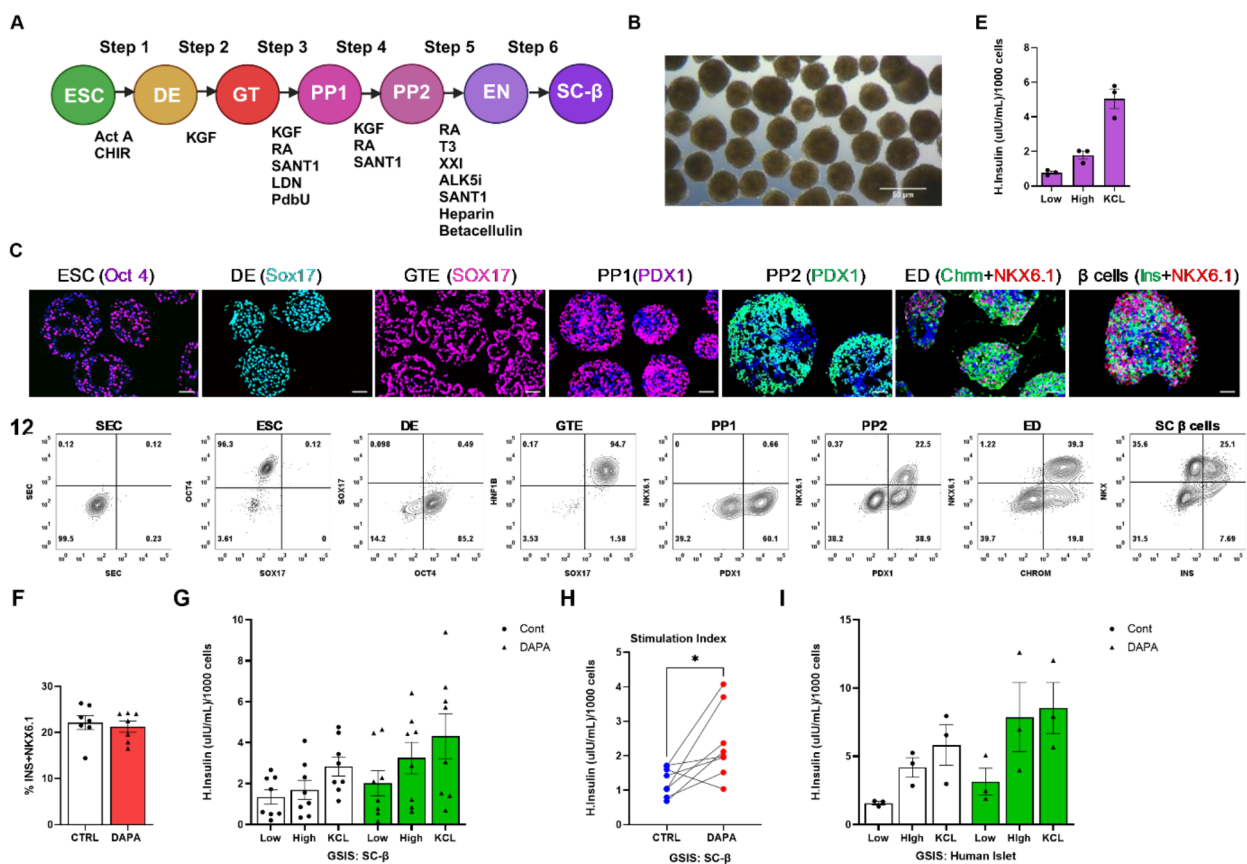


**Fig. 6** DAPA improves the insulin functionality of SC-β cells. **A** Representative image of the directed differentiation protocol for SC-β cells in-vitro. **B** A representative image of a fully developed SC-β cluster at step 6 (4x magnification). **C-D** Flow cytometry and immunofluorescence (IF) images for all stages, from embryonic stem cells (ESC), definitive endoderm (DE), gut tube endoderm (GTE), pancreatic progenitor 1, pancreatic progenitor 2, endocrine (ED), to stem cell-derived beta (SC-β) cells. **E** Glucose-stimulated insulin secretion (GSIS) of SC-β clusters. **F** Counting of insulin and NKX6.1-positive cells using flow cytometry. **G-H** GSIS ELISA measurement of SC-β between control and DAPA-treated groups, along with stimulation index measurement. **I** GSIS of human islets in control and DAPA treatment measured by ELISA. Error bars represent the standard error of the mean. Statistical significance is denoted as \* $p < 0.05$ , \*\* $p < 0.01$ , \*\*\* $p < 0.001$ , \*\*\*\* $p < 0.0001$

augment SC-β cell proliferation. Nevertheless, our study did not reveal significant variations in Ki67 (a marker of proliferation Kiel 67) expression post-DAPA treatment (Fig. 7A and B). It's worth noting that our experimental window was confined to 24 h, and prolonged exposure to DAPA could have yielded divergent findings.

Next, we conducted gene expression analyses to delve deeper into the effects of DAPA treatment on SC-β cells. Specifically, we examined the expression of key genes related to β-cell functions, including insulin, MAFA (MAF BZIP Transcription Factor A), GLUT1, and GLUT2 (Fig. 7C).

Our results revealed a significant increase in MAFA expression in the DAPA-treated group compared to control ( $p=0.017$ ). This finding aligns with the observed enhancement in the SC-β cells stimulation index shown in Fig. 7H, suggesting a potential mechanistic link. MAFA plays a pivotal role as a transcription factor involved in regulating insulin gene expression within SC-β cells. Its expression intricately governs GSIS, serving as a vital mediator of glucose-responsive insulin release from SC-β cells [76, 77]. Furthermore, our analyses demonstrated elevated levels of PI3K ( $p=0.0166$ )

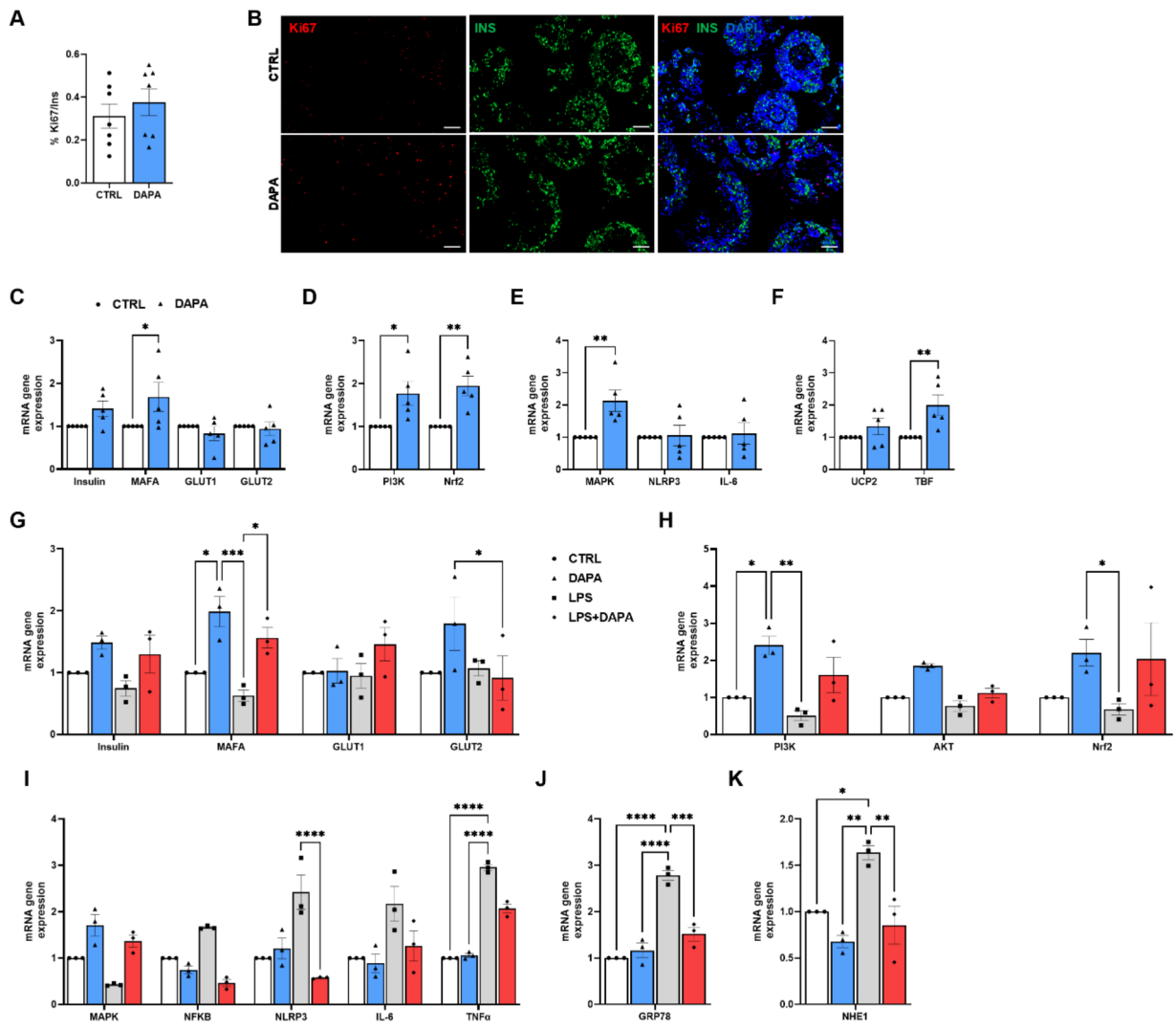


**Fig. 7** DAPA modulates SC-β cell function, inflammation, and stress response. **A-B** Representative images of cell counting and immunofluorescence and for Ki67. **C-F** mRNA gene expression of β-cell-related markers (Insulin, MAFA, GLUT1, and GLUT2) (**C**), AKT pathway-related genes (PI3K, NRF2) (**D**), inflammation-related pathways (MAPK, NLRP3, IL-6) (**E**), and mitochondria-related genes (XBP1, IRE-1, and GRP78) (**F**) in control and DAPA-treated groups. (**G-K**) mRNA gene expression of β-cell-related markers (Insulin, MAFA, GLUT1, and GLUT2) (**G**), AKT pathway-related genes (PI3K, AKT, and NRF2) (**H**), inflammatory and antioxidant genes (MAPK, NF-κB, NLRP3, IL-6, and TNFα) (**I**), GRP78 (**J**), and NHE-1 (**K**) comparing control, DAPA-treated, LPS-stimulated, and LPS + DAPA co-treated groups. Immunofluorescence staining images were captured at 10x and 20x magnification, with scale bars set at 100 μm. Error bars represent the standard error of the mean. Statistical significance is denoted as \* $p < 0.05$ , \*\* $p < 0.01$ , \*\*\* $p < 0.001$ , \*\*\*\* $p < 0.0001$

and NRF2 ( $p=0.0037$ ) in the DAPA-treated SC- $\beta$  cells compared to control groups (Fig. 7D). It's worth noting that PI3K indirectly influences NRF2 activity through its downstream effector AKT, which modulates NRF2 activation by inhibiting the degradation pathway involving GSK-3 $\beta$  [78–80].

We expanded our investigations to include genes associated with inflammation, such as MAPK, NLRP3, and IL6 (Fig. 7E), as well as mitochondria genes UCP2 and TBF (Fig. 7F). Our analysis revealed a significant increase in TBF in the treated group ( $p=0.0054$ ) compared to the control group. Further significant increase in MAPK ( $p=0.0059$ ) and GRP78 ( $p<0.0001$ ) expression in the DAPA-treated group compared to control. Given that MAPK regulates inflammation and GPR78 response to ER stress, the MAPK/ GPR78 interaction can influence cell fate and inflammation. It's known that when activated by stress signals, GPR78 can trigger downstream signaling pathways, including those involving PI3K and NF- $\kappa$ B. Dysregulation of these pathways is implicated in inflammatory disorders [80–82].

Our investigation aimed to understand the impact of DAPA on SC- $\beta$  cells within an inflammatory context based on our observation of DAPA's potential to influence inflammatory pathways as indicated by the DAPA-induced augmentation of MAPK expression. To induce inflammation, we stimulated  $\beta$ -cells with LPS [83–85]. Subsequently, we assessed the expression of crucial SC- $\beta$  cell-related genes, such as insulin, MAFA, GLUT1, and GLUT2 (Fig. 7G). While the other gene expressions remained unchanged, there was a notable elevation in MAFA expression in the DAPA-treated group compared to control ( $p=0.035$ ), reinforcing the DAPA's role in inducing SC- $\beta$  cell expression. Interestingly, MAFA expression decreased significantly after LPS stimulation compared to DAPA group ( $p<0.01$ ), while the MAFA expression increased again when LPS was combined with DAPA ( $p<0.05$  for LPS-alone compared to LPS+DAPA, Fig. 7G). Similarly, we observed increased expression of PI3K ( $p=0.001$ ) and NRF2 ( $p=0.04$ ) in the DAPA-treated group compared to the LPS-alone group (Fig. 7H). Both genes showed significantly reduced expression after LPS treatment compared to the DAPA-treated group, but an increase after LPS+DAPA treatment, although these changes were not statistically significant (on comparing the LPS-alone group to the LPS+DAPA group). There were no observed differences in AKT gene expression among all groups (Fig. 7H). While PI3K typically activates AKT, factors like phosphorylation status and feedback mechanisms may influence AKT activity independently of PI3K expression levels [86]. Further research is needed to understand the precise regulatory mechanisms at play in this discrepancy.

In addition to our previous findings, we conducted a comprehensive analysis of inflammatory and anti-inflammatory gene expressions (Fig. 7I). Consistent with our observations in cardiomyocytes and AECs, we detected a significant increase in NLRP3 expression following LPS stimulation compared to control as well as DAPA-alone groups. However, this elevation was notably diminished in the LPS+DAPA group ( $p<0.0001$  for LPS-alone vs. LPS+DAPA group), suggesting a robust inhibitory effect of DAPA on NLRP3 expression. This reinforces the notion of DAPA's potent action on NLRP3 across various cell types, as evidenced by the observed reduction in NLRP3 expression in cardiomyocytes undergoing hypertrophy, stimulated AECs, and stimulated SC- $\beta$  cells. These findings underscore the potential anti-inflammatory properties of DAPA, which could offer protection against conditions such as cardiac hypertrophy, endothelial inflammation, and pancreatic islet inflammation. Such effects hold promises for addressing conditions like cardiovascular diseases and diabetes.

Moreover, our investigations delved into the expression of another key inflammatory gene, TNF $\alpha$ , which exhibited a notable increase post-LPS stimulation ( $p<0.0001$  vs. control, and  $p<0.0001$  vs. DAPA-alone groups; Fig. 7I). Although we observed a reduction in TNF $\alpha$  expression upon DAPA treatment (i.e., LPS+DAPA group), this difference did not reach statistical significance. Interestingly, while DAPA seemed to primarily inhibit NLRP3 activation, its effects on other inflammatory genes were less pronounced. This variation could stem from DAPA's modulation of distinct stimuli or inflammatory pathways.

Furthermore, beyond inflammatory genes, NHE-1 assumes significance in inflammation due to its role in regulating the production of ROS, which is pivotal for inflammatory signaling in conditions like cardiovascular diseases. Given that the inhibition of NHE-1 can reduce oxidative stress and subsequent tissue damage [87, 88], we explored its expression in our study. Strikingly, our gene expression analysis unveiled a surge in NHE-1 expression following stimulation with LPS ( $p<0.05$  vs. control, and  $p<0.01$  vs. DAPA-alone group; Fig. 7K). However, this upregulation was markedly subdued following the addition of DAPA ( $p=0.004$  for LPS-alone vs. LPS+DAPA group). This suggests a potential mechanism whereby DAPA exerts its anti-inflammatory effects, offering new insights into its therapeutic implications for inflammatory conditions. Additionally, we investigated GRP78 expression, given its critical role in the ER stress response. Our findings showed a significant increase in GRP78 expression in the LPS-alone group ( $p<0.0001$  vs. control, and  $p<0.0001$  vs. DAPA-alone groups; Fig. 7J), which was significantly reduced with DAPA co-treatment ( $p=0.00055$  for LPS-alone group vs. LPS+DAPA

group). GRP78 is known to be upregulated during ER stress, being crucial in maintaining cellular homeostasis, promoting cell survival during stress, and ensuring proper protein folding and quality control [89]. However, in pathological conditions, its protective functions can become maladaptive, contributing to disease progression, resistance to treatment, and chronic inflammation [90, 91]. These findings emphasize the crucial role of DAPA in modulating stress genes such as GRP78, potentially mitigating the adverse effects associated with dysregulated cellular stress responses.

## Materials and methods

### Cell culture, treatment, and differentiation

#### *Cardiomyocytes*

AC16 human cardiomyocyte cell lines (ATCC, CRL-3568) were cultured following the manufacturer's instructions in DMEM F-12 medium, which was supplemented with 12.5% fetal bovine serum (ATCC, 30-2020), 1% penicillin-streptomycin (Gibco, R15140-122) and 1% L-glutamine (Corning, 25-015-CL). The culture media was replaced every 48 h. The cells were incubated at 37 °C with 5% CO<sub>2</sub>. AC16 cells were exposed to ISO at concentrations of 10 and 20 μM (Sigma, I6504) and treated with DAPA at concentrations of 0.5 and 1 μM (Sigma, SML2804) at various time points.

#### *Aortic endothelial cells (AECs)*

AECs (CC-2535, Lonza) were cultured in EBM™-2 Basal Medium (CC-3156, Lonza) supplemented with EGM™-2 SingleQuots™ from the EGM™-2 BulletKit™ (CC-3162, Lonza). The cells were maintained in an incubator at 37 °C with 5% CO<sub>2</sub>, with the media changed every 48 h. To induce an inflammatory condition, the cells were treated with 100 ng/ml of TNFα (R&D, 210-TA-020) and subsequently exposed to 1 μM DAPA for 24 h.

#### *Stem cell-derived β (SC-β) cells*

Human pluripotent stem cell maintenance and differentiation were conducted as previously described [73]. Stem cells were adapted to a 3D culture system using 500 mL spinner flasks (Corning, 3153) and maintained in mTeSR media (Stem Cell Technologies Inc., 24243). Suspension cultures were established by seeding 150 million cells in mTeSR media with 10 μM Y27632 (R&D Systems, 4448) and maintained at 70 rpm in a humidified incubator at 37 °C with 5% CO<sub>2</sub>. The media was changed every 48 h, and the cells were passaged every 72 h by dispersing to single cells using Accutase (Sigma Aldrich, A6964-500ML). Freshly split cells were seeded into fresh mTeSR with Y27632. SC-β cells were sequentially directed from definitive endoderm to mature and functional β-cells (stages 1–6) as previously described [73]. After maturation to β-cells, the cells were treated with 0.5 μM DAPA

and 20 ng/ml LPS for 24 h. Stimulated cells were collected after 24 h for flow cytometry, IF, and PCR analysis. The Mayo Clinic Stem Cell Research Committee approved all work involving human pluripotent stem cells.

#### *Cell viability assessment*

The MTT assay was used to assess the cardiomyocyte viability (Cayman Chemical, 10009365). The AC16 cardiomyocytes were incubated for three hours in DMEM containing 0.5 mg/mL MTT. The incubation buffer was removed, and the blue MTT-formazan product was extracted with dimethyl sulfoxide (DMSO). The absorbance of the formazan solution was read spectrophotometrically at 570 nm.

#### *ROS measurement*

AC16 cardiomyocytes were pre-treated with or without DAPA for two hours. Next, the cells were stimulated with ISO for 24 h to generate ROS. After removing the medium, the cells were washed twice with phosphate-buffered saline (PBS) and incubated with 10 μM DCFHDA for 25 min. DCFHDA was used to determine the ROS generation in the cardiomyocytes. The stained cardiomyocytes were then analyzed using a FACS Aria flow cytometer.

#### *Glucose stimulated insulin secretion (GSIS) assay*

##### *GSIS protocol*

SC-β cells were washed twice in low-glucose (2.8 mM) Krebs Ringer (KRB) buffer and then loaded into 24-well transwell inserts. The cells were fasted in low-glucose KRB for 1 h at 37 °C. After fasting, the clusters were washed once in low-glucose KRB and incubated in low-glucose KRB for another hour at 37 °C. Subsequently, the cells were transferred to high-glucose KRB (20 mM) for 1 h at 37 °C, followed by a transfer to low-glucose KRB with 30 mM KCl for 1 h at 37 °C. Supernatants were collected at each transfer for insulin measurement. To study the efficacy of DAPA (0.5 μM) on SC-β cells treated with 100 ng/ml LPS, the cells were placed on a rocker in the incubator for 24 h. After this treatment, the cells were dispersed using TrypLE, and cell counts were determined using a ViCELL automated cell counter. Human insulin levels were measured using an enzyme-linked immunosorbent assay (ELISA) kit.

#### *ELISA*

The supernatant collected from the glucose challenge at different time points was diluted to 1:200 using KRB. The concentration of human insulin levels was quantified using the Human Ultrasensitive Insulin ELISA kit (Alpco, 80-INSHUU-E10). The secretion levels of IL-1β, IL-6, TNFα, ICAM-1, VCAM-1, and BNP were measured



in the cell supernatants from both control and treatment groups. Additionally, assays for eNOS, iNOS, and NOS activity were performed on cell homogenates. All assays were conducted following the manufacturer's instructions as detailed in Supplementary Table 3.

#### Flow cytometry

SC- $\beta$  cell clusters were collected for flow cytometry throughout the six differentiation stages. The clusters were dispersed using TrypLE Express (Thermo Fisher, 12563029) in a 37 °C water bath for 10 min and then quenched with S3 media. The cells were counted, fixed in 4% PAF (Millipore Sigma, 15710), and stored at 4 °C until staining. For staining, the cells were blocked in a donkey block solution for 40 min. They were subsequently incubated with primary antibodies for 1 h at room temperature (RT) or overnight at 4 °C. After incubation, the cells were washed three times with PBST (phosphate-buffered saline with Tween® detergent) and then incubated with secondary antibodies for 2 h at RT. Following three additional washes, the cells were re-suspended in PBST at a concentration of  $1 \times 10^6$  cells/mL. The stained cells were analyzed using the "Attune" flow cytometer. The data from flow cytometry were processed using FlowJo v10 and Attune NxT v4.2.6 software.

#### Immunofluorescence (IF)

##### Staining protocol

Cardiomyocytes, AECs, and SC- $\beta$  cell clusters were fixed in 4% PFA for 1 h at RT or overnight at 4 °C, then washed three times with PBS. The cell clusters were embedded in Histogel, while cardiomyocytes and AECs were stored in the cell culture plate in 4% PFA. Paraffin-embedded samples were treated with Histo-Clear to remove the paraffin. All slides were rehydrated through an ethanol gradient and incubated in boiling antigen retrieval reagent (10 mM sodium citrate, pH 6.0) for 60 min. The slides were then washed three times and incubated in a blocking donkey serum for 40 min. Sections were incubated with the primary antibody overnight at 4 °C, washed three times, and then incubated with a secondary antibody for 2 h at RT. After three additional washes, the slide sections were mounted using Fluoromount-G with DAPI (4', 6-diamidino-2-phenylindole). The plates and cluster sections were imaged using an EVOS-FL Auto-2 imaging station. IF images were captured with a Zeiss Axio Observer microscope and ZEN2 Blue software. The images shown are representative of similar results obtained from at least three separate biological samples. The antibodies used are listed in Supplementary Table 1.

##### Cell surface area measurement

AC16 cardiomyocytes were treated with 10 and 20  $\mu$ M isoproterenol (ISO; Sigma Chemical, St Louis, USA) for

24 h, then cells were fixed with 4% paraformaldehyde (PAF) and stained with wheat germ agglutinin (WGA). After washing with PBS for three times, cardiomyocytes were visualized under the inverted fluorescence microscope and 25 random individual cell surface areas from each well were measured by ImageJ software (National Institutes of Health, Bethesda, USA). AECs and SC- $\beta$  cells of interest were manually counted using a Zeiss Axio Observer microscope and ZEN2 Blue software.

#### Real-time polymerase chain reaction (RT-PCR)

Cardiomyocytes, AECs, and SC- $\beta$  cells were collected and stored at -80 °C for RNA isolation. Total RNA was purified using the RNeasy Mini Kit (QIAGEN, 74106) according to the manufacturer's protocol. Complementary (c)DNA was synthesized by reverse transcribing 400 ng of total RNA following the manufacturer's instructions (Biorad, 170-8891). Quantitative RT-PCR was performed in a 20  $\mu$ L reaction mixture containing 1  $\mu$ L of cDNA, 200 nM of each primer, and 10  $\mu$ L of SYBR Select Master Mix using the Applied Biosystems 7500 RT-PCR System (Applied Biosystem, 4368706). The used primer sequences are listed in Supplementary Table 2.

#### Western blot

After cell lysis, protein was extracted using a total protein extraction kit (Sigma, R0278), and the protein concentration was determined using a Bicinchoninic Acid (BCA) Protein Quantification Kit (Thermo Fisher, 23225). Total protein samples were loaded at 50  $\mu$ g/well onto a sodium dodecyl sulfate-polyacrylamide gel (SDS-PAGE) for electrophoresis and subsequently transferred to polyvinylidene fluoride membranes (Millipore, 03010040001). The membranes were incubated in a 5% BSA solution at RT for one hour. Then, they were treated with primary antibodies against the target proteins and  $\beta$ -actin, which served as the internal reference. The primary antibodies were incubated overnight at 4 °C, followed by washing with TBST, and then treatment with secondary antibodies. The secondary antibodies were incubated at RT for one hour followed by washing with TBST. Images were obtained with a LiCor Odyssey® Fc imager, and the gray values of the bands were analyzed using ImageJ software. The primary and secondary antibodies used in the experiment are listed in the Supplementary Table 2. All uncropped western blot protein expression images are shown in Supplementary Figs. 1,2 and 3.

#### Statistical analysis

The data analyses were conducted using the GraphPad Prism v.10.3.1 software. The students' t-test was used to compare the means between the two groups. For comparing means of multiple groups, one-way and two-way ANOVA (analysis of variance) with multiple comparison

tests were utilized. A p-value of less than 0.05 was considered statistically significant.

## Discussion

This comprehensive study on the effects of DAPA on various cellular processes in cardiomyocytes, AECs, and SC- $\beta$  cells has yielded multifaceted insights into its therapeutic potential across different cell types. The findings from this investigation shed light on DAPA's diverse mechanisms of action, ranging from its impact on cellular hypertrophy and inflammation to its modulation of insulin functionality and stress response genes [12, 28, 29].

In the context of cardiomyocyte hypertrophy, our study elucidated, through experimentation involving co-treatment and post-stimulation conditions, the ability of DAPA to mitigate hypertrophic stimuli induced by ISO, which is a  $\beta$ -adrenergic receptor agonist known to induce cardiomyocyte hypertrophy [9, 92]. Notably, DAPA's protective effects were associated with reductions in ROS levels and inflammation, primarily mediated by the upgrading of the AKT pathway. By activating AKT signaling, DAPA not only counteracted hypertrophy but also curbed inflammation and oxidative stress, thus safeguarding cardiomyocyte functions [9–12]. In ISO-induced cardiomyocyte hypertrophy, DAPA treatment led to several positive outcomes, including increased AKT expression, decreased ROS levels, and reduced levels of fibrosis (SMAD) and hypertrophy (ANP and BNP) markers and inflammatory cytokines. Interestingly, while SGLT2 activation persisted after the ISO challenge, its gene and protein expression decreased following DAPA treatment, suggesting a potential role of DAPA in modulating SGLT2 expression. This phenomenon was consistently observed in both stimulated cardiomyocytes and AECs. One plausible connection is that DAPA, known for its SGLT2 inhibitory effects, may interfere with SGLT2-mediated glucose reabsorption pathways. This interference could potentially delay glucose reabsorption, impacting inflammatory pathways associated with glucose metabolism in cardiovascular cells. Moreover, the observed reduction in downstream NHE1 activity upon DAPA treatment suggests a broader impact. It hints that DAPA might not only influence SGLT2 but also affect NHE1 function directly or through modulation via the AKT pathway. This modulation could potentially alter ion transporter activity, thereby contributing to enhanced cardiovascular and metabolic health outcomes in the context of cardiomyocyte hypertrophy and related conditions [39, 40]. Moreover, the increase in NRF2 and decrease in NLRP3 levels with DAPA treatment indicates its antioxidant and anti-inflammatory capacities. The activation of the AKT pathway by DAPA played a crucial role in reducing hypertrophy, fibrosis, and inflammation;

thus, enhancing the cardiomyocyte functions by improving cell survival and decreasing oxidative stress. In line with these results, previous studies have indicated that DAPA can improve cardiac function in animal models of myocardial infarction and diabetes by affecting the PI3K/AKT axis [10]. Our research, for the first time, suggests that the DAPA's impact on AKT-related pathways in ISO-induced cardiomyocytes might shed light on these mechanisms.

Several studies have examined the effects of DAPA on endothelial cells [12, 16, 93–95], but its specific actions on aortic endothelial cells (AECs) have been less well-studied. AECs are integral to cardiovascular health, regulating vascular tone, mediating responses to oxidative stress, and maintaining antithrombotic and anti-inflammatory properties. Dysfunction in AECs contributes to hypertension, atherosclerosis, and increased thrombotic risk, all of which are significant factors in cardiovascular diseases [96–98]. In our study, AECs stimulated with TNF $\alpha$  revealed that DAPA significantly reduced inflammatory markers, likely through activation of the AKT/PI3K and MAPK pathways, which are critical in cellular survival and inflammation regulation. This reduction in inflammatory signaling highlights DAPA's ability to counteract the deleterious effects of TNF $\alpha$ , thereby preserving AEC function and mitigating vascular inflammation. Furthermore, DAPA's regulation of adhesion molecules such as ICAM-1 and VCAM-1, as well as glucose transporters, underscores its broader role in preventing endothelial dysfunction. By reducing the expression of these adhesion molecules, DAPA may limit leukocyte recruitment and the progression of atherosclerosis, highlighting its potential protective effect on vascular integrity. Importantly, DAPA also modulated glucose transporters like GLUT1, indicating an additional metabolic benefit that may support endothelial function under stress conditions. In combination with ISO, DAPA showed a significant synergistic effect in regulating endothelial function, particularly through modulation of eNOS, iNOS, and NO levels. Both treatments enhanced eNOS expression, increasing NO bioavailability, which is essential for vasodilation and endothelial homeostasis [67]. The reduction in iNOS levels further suggests anti-inflammatory effects by curbing excessive NO production linked to oxidative stress. The combined influence of ISO and DAPA on total NO levels points to their ability to restore NO balance, a critical factor in maintaining vascular health and preventing endothelial dysfunction. These findings collectively suggest that ISO and DAPA co-treatment not only preserves endothelial function but also offers potential therapeutic benefits for addressing inflammation-driven cardiovascular conditions, particularly in the context of metabolic stress and chronic inflammation. This dual regulatory effect on both inflammation and metabolism

positions DAPA as a promising candidate for the treatment of cardiovascular diseases where endothelial dysfunction is a key pathological feature.

Expanding its scope to SC- $\beta$  cells, the study unveiled DAPA's intriguing effects on insulin functionality and stress response genes. While DAPA did not alter the identity of SC- $\beta$  cells, it significantly enhanced their insulin functionality, potentially through upregulation of MAFA expression and elevated PI3K and NRF2 levels, which are crucial transcription factors involved in insulin regulation. Despite SGLT2 are not expressed in  $\beta$ -cells [21, 22], DAPA still reduced inflammatory markers including NLRP3, suggesting that the beneficial effects of DAPA are mediated through systemic metabolic improvements, paracrine signaling, or alternative pathways such as PI3K and NRF2 [10, 45]. The consistent reduction of NLRP3 and other inflammatory markers across all cell types studied, regardless of the inflammatory stimulus used, highlights a systemic anti-inflammatory effect of DAPA. The increase in NRF2 expression across different cell types indicates a central role of NRF2 in mediating DAPA's antioxidant and anti-inflammatory effects [10, 99]. The enhancement of the AKT pathway in cardiomyocytes and AECs, along with the indirect action on SC- $\beta$  cells through PI3K and NRF2, underscores the multifaceted mechanisms through which DAPA exerts its protective effects.

All three cell types of cardiomyocytes, AECs, and SC- $\beta$  cells exhibited activation of the AKT pathway, demonstrating a common mechanism through which DAPA exerts its therapeutic effects. This common activation suggests that DAPA's role in enhancing AKT signaling might be a key factor in its ability to mitigate inflammation, oxidative stress, and cellular dysfunction across different tissues. The activation of the AKT pathway across these cell types not only highlights DAPA's broad therapeutic potential but also underscores its capacity to target fundamental cellular processes involved in disease progression. By modulating AKT signaling, DAPA effectively addresses the core pathological mechanisms in diverse cell types, which could translate to comprehensive clinical benefits in treating conditions like heart disease, diabetes, and metabolic syndrome. Overall, our findings demonstrate that DAPA's benefits extend beyond glucose lowering, involving the activation of the AKT pathway and reduction of hypertrophy, fibrosis, and inflammation in cardiomyocytes, AECs, and SC- $\beta$  cells. These results underscore DAPA's therapeutic potential in treating cardiovascular and metabolic diseases by targeting multiple pathways to reduce inflammation and improve cell survival.

Despite the promising findings elucidating the multifaceted effects of DAPA on cardiomyocytes, AECs, and SC- $\beta$  cells, some limitations warrant consideration. In

the current study, our primary focus was only to investigate the impact of DAPA treatment on these three different cell types to determine whether they exhibit similar responses in terms of activating molecular pathways (such as AKT) and inflammation when exposed to stimuli. However, the complexity of cellular interactions and signaling pathways suggests that translating these findings to in-vivo models is essential to assess their clinical relevance. Additionally, the study primarily focused on the acute effects of DAPA treatment, necessitating further investigations into its long-term implications. Chronic exposure to DAPA may lead to different cellular adaptations and responses, which could have significant implications for its therapeutic use in conditions such as diabetes and cardiovascular diseases. So, long-term studies are imperative to evaluate the sustained effects of DAPA and to identify any potential adverse effects or limitations associated with prolonged treatment.

## Conclusion

This comprehensive study highlights the diverse mechanisms through which DAPA exerts its effects across three different cell types. By elucidating its role in cellular hypertrophy, inflammation, vascular signaling, insulin functionality, and stress responses, our research positions DAPA as a promising therapeutic agent with broad-spectrum efficacy. These findings provide a solid foundation for future investigations aimed at harnessing DAPA's therapeutic benefits for improving cardiovascular diseases and metabolic inflammatory syndromes. However, further research is essential to validate these findings in in vivo models, which will be crucial for translating these results into clinical applications.

## Supplementary Information

The online version contains supplementary material available at <https://doi.org/10.1186/s12933-024-02481-y>.

Supplementary Material 1

Supplementary Material 2

Supplementary Material 3

Supplementary Material 4

## Acknowledgements

We gratefully acknowledge the financial support provided by the Khalifa Bin Zayed Al Nahyan Foundation (KBZF). This support was essential for the successful completion of this project. We also wish to specifically acknowledge the invaluable contributions of His Excellency Mohammed Haji AlKhoori, General Director of the KBZF in the United Arab Emirates, and Amira Almutawa, Head of the Health Program.

## Author contributions

F.R.A, Z.K., A.M.A., M.M.R., Q.P.P and M.A.S. designed the study. F.R.A, Z.K., A.M.A., T.S. M.K.A, M.M.M., A. M.H., H.M. and M.A.S. collected and sorted statistical data. All authors discussed the results and wrote the paper. All authors read and approved the final manuscript.

Targeted Research Project, Grant No. (23010902135): from University of Sharjah, Sharjah, United Arab Emirates. Khalifa Bin Zayed Al Nahyan Foundation (KBZF).

**Data availability**

No datasets were generated or analysed during the current study.

**Declarations**

**Competing interests**

The authors declare no competing interests.

**Author details**

<sup>1</sup>Cardiovascular Research Group, Research Institute for Medical and Health Sciences, University of Sharjah, Sharjah 27272, United Arab Emirates

<sup>2</sup>Department of Physiology and Biomedical Engineering, Mayo Clinic, Rochester, MN, USA

<sup>3</sup>Emirates Health Services (EHS), Dubai, United Arab Emirates

<sup>4</sup>College of Medicine and Health Sciences, United Arab Emirates University, Abu Dhabi, United Arab Emirates

<sup>5</sup>Endocrinology and Metabolism Department, Armed Forces College of Medicine, Cairo, Egypt

<sup>6</sup>Department of Clinical Sciences, College of Medicine, University of Sharjah, Sharjah, United Arab Emirates

<sup>7</sup>Department of Cardiology, Faculty of Medicine, Mansoura University, Mansoura 35516, Egypt

<sup>8</sup>Center for Regenerative Medicine, Mayo Clinic, Rochester, MN, USA

<sup>9</sup>Department of Pharmacology and Toxicology, Faculty of Pharmacy, Mansoura University, Mansoura 35516, Egypt

Received: 28 July 2024 / Accepted: 21 October 2024

Published online: 29 October 2024

**References**

1. Alhusaini AM, Alghibiwi HK, Sarawi WS, Alsaab JS, Alshehri SM, Alqahtani QH, Alshaniwani AR, Aljassas EA, Alsaltan EN, Hasan IH. Resveratrol-based liposomes improve cardiac remodeling induced by isoproterenol partially by modulating MEF2, cytochrome C and S100A1 expression. *Dose Response*. 2024;22:15593258241247980. <https://doi.org/10.1177/15593258241247980>.
2. Parreira RC, Gómez-Mendoza DP, de Jesus ICG, Lemos RP, Santos AK, Rezende CP, Figueiredo HCP, Pinto MCX, Kjeldsen F, Guatimosim S, et al. Cardiomyocyte proteome remodeling due to isoproterenol-induced cardiac hypertrophy during the compensated phase. *Proteom Clin Appl*. 2020;14:e2000017. <https://doi.org/10.1002/prca.202000017>.
3. Bai L, Kee HJ, Han X, Zhao T, Kee SJ, Jeong MH. Protocatechuic acid attenuates isoproterenol-induced cardiac hypertrophy via downregulation of ROCK1-Sp1-PKC $\gamma$  axis. *Sci Rep*. 2021;11:17343. <https://doi.org/10.1038/s41598-021-96761-2>.
4. Zinman B, Lachin JM, Inzucchi SE. Empagliflozin, Cardiovascular outcomes, and mortality in type 2 diabetes. *N Engl J Med*. 2016;374:1094. <https://doi.org/10.1056/NEJMc1600827>.
5. Fitchett D, Zinman B, Wanner C, Lachin JM, Hantel S, Salsali A, Johansen OE, Woerle HJ, Broedl UC, Inzucchi SE. Heart failure outcomes with empagliflozin in patients with type 2 diabetes at high cardiovascular risk: results of the EMPA-REG OUTCOME<sup>®</sup> trial. *Eur Heart J*. 2016;37:1526–34. <https://doi.org/10.1093/eurheartj/ehv728>.
6. Anitha AP, Balasubramanian S, Ramalingam AG, Samuel Kennady SR, Ganamurali N, Dhanasekaran D, Sabarathinam S. An exploration of the experience of dapagliflozin in clinical practice. *Future Sci OA*. 2022;8:Fso816. <https://doi.org/10.2144/fsoa-2022-0038>.
7. Fatima A, Rasool S, Devi S, Talha M, Waqar F, Nasir M, Khan MR, Ibne Ali Jaffari SM, Haider A, Shah SU, et al. Exploring the cardiovascular benefits of sodium-glucose cotransporter-2 (SGLT2) inhibitors: expanding horizons beyond diabetes management. *Cureus*. 2023;15:e46243. <https://doi.org/10.7759/cureus.46243>.
8. Hasan I, Rashid T, Jaikaransingh V, Heilig C, Abdel-Rahman EM, Awad AS. SGLT2 inhibitors: beyond glycemic control. *J Clin Transl Endocrinol*. 2024;35:100335. <https://doi.org/10.1016/j.jcte.2024.100335>.

9. Yang ZJ, Guo CL, Gong YX, Li L, Wang LL, Liu HM, Cao JM, Lu ZY. Dapagliflozin suppresses isoprenaline-induced cardiac hypertrophy through inhibition of mitochondrial fission. *J Cardiovasc Pharmacol*. 2024;83:193–204. <https://doi.org/10.1097/fjc.0000000000001518>.
10. Hsieh PL, Chu PM, Cheng HC, Huang YT, Chou WC, Tsai KL, Chan SH. Dapagliflozin mitigates doxorubicin-caused myocardium damage by regulating AKT-mediated oxidative stress, cardiac remodeling, and inflammation. *Int J Mol Sci*. 2022;23. <https://doi.org/10.3390/ijms231710146>.
11. Han X, Liu X, Zhao X, Wang X, Sun Y, Qu C, Liang J, Yang B. Dapagliflozin ameliorates sepsis-induced heart injury by inhibiting cardiomyocyte apoptosis and electrical remodeling through the PI3K/Akt pathway. *Eur J Pharmacol*. 2023;955:175930. <https://doi.org/10.1016/j.ejphar.2023.175930>.
12. Alsereidi FR, Khashim Z, Marzook H, Gupta A, Al-Rawi AM, Ramadan MM, Saleh MA. Targeting inflammatory signaling pathways with SGLT2 inhibitors: insights into cardiovascular health and cardiac cell improvement. *Curr Probl Cardiol*. 2024;49:102524. <https://doi.org/10.1016/j.cpcardiol.2024.102524>.
13. Hers I, Vincent EE, Tavaré JM. Akt signalling in health and disease. *Cell Signal*. 2011;23:1515–27. <https://doi.org/10.1016/j.cellsig.2011.05.004>.
14. Chaanine AH, Hajjar RJ. Akt signalling in the failing heart. *Eur J Heart Fail*. 2011;13:825–9. <https://doi.org/10.1093/eurjhf/hfr080>.
15. El-Sayed N, Mostafa YM, AboGresha NM, Ahmed AAM, Mahmoud IZ, El-Sayed NM. Dapagliflozin attenuates diabetic cardiomyopathy through erythropoietin up-regulation of AKT/JAK/STAT3 pathways in streptozotocin-induced diabetic rats. *Chem Biol Interact*. 2021;347:109617. <https://doi.org/10.1016/j.cb.2021.109617>.
16. Ma L, Zou R, Shi W, Zhou N, Chen S, Zhou H, Chen X, Wu Y. SGLT2 inhibitor dapagliflozin reduces endothelial dysfunction and microvascular damage during cardiac ischemia/reperfusion injury through normalizing the XO-SERCA2-CaMKII-cofilin pathways. *Theranostics*. 2022;12:5034–50. <https://doi.org/10.7150/thno.75121>.
17. Li X, Preckel B, Hermanides J, Hollmann MW, Zuurbier CJ, Weber NC. Amelioration of endothelial dysfunction by sodium glucose co-transporter 2 inhibitors: pieces of the puzzle explaining their cardiovascular protection. *Br J Pharmacol*. 2022;179:4047–62. <https://doi.org/10.1111/bph.15850>.
18. Scheen AJ. Pharmacokinetic and pharmacodynamic profile of empagliflozin, a sodium glucose co-transporter 2 inhibitor. *Clin Pharmacokinet*. 2014;53:213–25. <https://doi.org/10.1007/s40262-013-0126-x>.
19. Inzucchi SE, Zinman B, Wanner C, Ferreri R, Fitchett D, Hantel S, Espadero RM, Woerle HJ, Broedl UC, Johansen OE. SGLT-2 inhibitors and cardiovascular risk: proposed pathways and review of ongoing outcome trials. *Diab Vasc Dis Res*. 2015;12:90–100. <https://doi.org/10.1177/1479164114559852>.
20. Wei R, Cui X, Feng J, Gu L, Lang S, Wei T, Yang J, Liu J, Le Y, Wang H, et al. Dapagliflozin promotes beta cell regeneration by inducing pancreatic endocrine cell phenotype conversion in type 2 diabetic mice. *Metabolism*. 2020;111:154324. <https://doi.org/10.1016/j.metabol.2020.154324>.
21. Chae H, Augustin R, Gatineau E, Mayoux E, Bensellam M, Antoine N, Khattab F, Lai BK, Brusa D, Stierstorfer B, et al. SGLT2 is not expressed in pancreatic  $\alpha$ - and  $\beta$ -cells, and its inhibition does not directly affect glucagon and insulin secretion in rodents and humans. *Mol Metab*. 2020;42:101071. <https://doi.org/10.1016/j.molmet.2020.101071>.
22. Nakamura A. Effects of Sodium-glucose co-transporter-2 inhibitors on pancreatic  $\beta$ -Cell Mass and function. *Int J Mol Sci*. 2022;23. <https://doi.org/10.3390/ijms23095104>.
23. Kajimoto Y, Kaneto H. Role of oxidative stress in pancreatic beta-cell dysfunction. *Ann NY Acad Sci*. 2004;1011:168–76. [https://doi.org/10.1007/978-3-662-41088-2\\_17](https://doi.org/10.1007/978-3-662-41088-2_17).
24. Hill JA, Olson EN. Cardiac plasticity. *N Engl J Med*. 2008;358:1370–80. <https://doi.org/10.1056/NEJMra072139>.
25. Drazner MH. The progression of hypertensive heart disease. *Circulation*. 2011;123:327–34. <https://doi.org/10.1161/circulationaha.108.845792>.
26. Wiviott SD, Raz I, Bonaca MP, Mosenzon O, Kato ET, Cahn A, Silverman MG, Zelniker TA, Kuder JF, Murphy SA, et al. Dapagliflozin and Cardiovascular outcomes in type 2 diabetes. *N Engl J Med*. 2019;380:347–57. <https://doi.org/10.1056/NEJMoa1812389>.
27. Zelniker TA, Wiviott SD, Raz I, Im K, Goodrich EL, Bonaca MP, Mosenzon O, Kato ET, Cahn A, Furtado RHM, et al. SGLT2 inhibitors for primary and secondary prevention of cardiovascular and renal outcomes in type 2 diabetes: a systematic review and meta-analysis of cardiovascular outcome trials. *Lancet*. 2019;393:31–9. [https://doi.org/10.1016/s0140-6736\(18\)32590-x](https://doi.org/10.1016/s0140-6736(18)32590-x).
28. Liu T, Wu J, Shi S, Cui B, Xiong F, Yang S, Yan M. Dapagliflozin attenuates cardiac remodeling and dysfunction in rats with  $\beta$ -adrenergic receptor overactivation through restoring calcium handling and suppressing cardiomyocyte



- apoptosis. *Diab Vasc Dis Res.* 2023;20:14791641231197106. <https://doi.org/10.1177/14791641231197106>.
29. Gao W, Guo N, Yan H, Zhao S, Sun Y, Chen Z. MycN ameliorates cardiac hypertrophy-induced heart failure in mice by mediating the USP2/JUP/Akt/ $\beta$ -catenin cascade. *BMC Cardiovasc Disord.* 2024;24:82. <https://doi.org/10.1186/s12872-024-03748-8>.
30. Uthman L, Homayr A, Juni RP, Spin EL, Kerindongo R, Boomsma M, Hollmann MW, Preckel B, Koolwijk P, van Hinsbergh WVM, et al. Empagliflozin and Dapagliflozin reduce ROS Generation and restore NO bioavailability in Tumor necrosis factor  $\alpha$ -Stimulated human coronary arterial endothelial cells. *Cell Physiol Biochem.* 2019;53:865–86. <https://doi.org/10.33594/000000178>.
31. Durak A, Olgar Y, Degirmenci S, Akkus E, Tuncay E, Turan B. A SGLT2 inhibitor dapagliflozin suppresses prolonged ventricular-repolarization through augmentation of mitochondrial function in insulin-resistant metabolic syndrome rats. *Cardiovasc Diabetol.* 2018;17:144. <https://doi.org/10.1186/s12933-018-0790-0>.
32. Peng TI, Jou MJ. Oxidative stress caused by mitochondrial calcium overload. *Ann N Y Acad Sci.* 2010;1201:183–8. <https://doi.org/10.1111/j.1749-6632.2010.05634.x>.
33. DeBosch B, Treskov I, Lupu TS, Weinheimer C, Kovacs A, Courtois M, Muslin AJ. Akt1 is required for physiological cardiac growth. *Circulation.* 2006;113:2097–104. <https://doi.org/10.1161/circulationaha.105.595231>.
34. Shioi T, Kang PM, Douglas PS, Hampe J, Yballe CM, Lawitts J, Cantley LC, Izumo S. The conserved phosphoinositide 3-kinase pathway determines heart size in mice. *Embo J.* 2000;19:2537–48. <https://doi.org/10.1093/emboj/19.11.2537>.
35. Madrid LV, Wang CY, Guttridge DC, Schottelius AJ, Baldwin AS Jr, Mayo MW. Akt suppresses apoptosis by stimulating the transactivation potential of the RelA/p65 subunit of NF- $\kappa$ B. *Mol Cell Biol.* 2000;20:1626–38. <https://doi.org/10.1128/mcb.20.5.1626-1638.2000>.
36. Chang WT, Shih JY, Lin YW, Chen ZC, Kan WC, Lin TH, Hong CS. Dapagliflozin protects against doxorubicin-induced cardiotoxicity by restoring STAT3. *Arch Toxicol.* 2022;96:2021–32. <https://doi.org/10.1007/s00204-022-03298-y>.
37. Zaibi N, Li P, Xu SZ. Protective effects of dapagliflozin against oxidative stress-induced cell injury in human proximal tubular cells. *PLoS ONE.* 2021;16:e0247234. <https://doi.org/10.1371/journal.pone.0247234>.
38. Deng RM, Zhou J. The role of PI3K/AKT signaling pathway in myocardial ischemia-reperfusion injury. *Int Immunopharmacol.* 2023;123:110714. <https://doi.org/10.1016/j.intimp.2023.110714>.
39. Uthman L, Baartscheer A, Bleijlevens B, Schumacher CA, Fiolet JWT, Koeman A, Jancev M, Hollmann MW, Weber NC, Coronel R, et al. Class effects of SGLT2 inhibitors in mouse cardiomyocytes and hearts: inhibition of Na<sup>(+)</sup>/H<sup>(+)</sup> exchanger, lowering of cytosolic Na<sup>(+)</sup> and vasodilation. *Diabetologia.* 2018;61:722–6. <https://doi.org/10.1007/s00125-017-4509-7>.
40. Chen S, Coronel R, Hollmann MW, Weber NC, Zuurbier CJ. Direct cardiac effects of SGLT2 inhibitors. *Cardiovasc Diabetol.* 2022;21:45. <https://doi.org/10.1186/s12933-022-01480-1>.
41. Madonna R, Biondi F, Alberti M, Ghelardoni S, Mattioli L, D'Alleva A. Cardiovascular outcomes and molecular targets for the cardiac effects of sodium-glucose cotransporter 2 inhibitors: a systematic review. *Biomed Pharmacother.* 2024;175:116650. <https://doi.org/10.1016/j.biopha.2024.116650>.
42. Orłowski J, Grinstein S. Na<sup>(+)</sup>/H<sup>(+)</sup> exchangers of mammalian cells. *J Biol Chem.* 1997;272:22373–6. <https://doi.org/10.1074/jbc.272.36.22373>.
43. Peshavariya H, Dusting GJ, Jiang F, Halmos LR, Sobey CG, Drummond GR, Selemidis S. NADPH oxidase isoform selective regulation of endothelial cell proliferation and survival. *Naunyn Schmiedeberg's Arch Pharmacol.* 2009;380:193–204. <https://doi.org/10.1007/s00210-009-0413-0>.
44. Verma S, McMurray JJV. SGLT2 inhibitors and mechanisms of cardiovascular benefit: a state-of-the-art review. *Diabetologia.* 2018;61:2108–17. <https://doi.org/10.1007/s00125-018-4670-7>.
45. Wang L, Chen Y, Sternberg P, Cai J. Essential roles of the PI3 kinase/Akt pathway in regulating Nrf2-dependent antioxidant functions in the RPE. *Invest Ophthalmol Vis Sci.* 2008;49:1671–8. <https://doi.org/10.1167/iov.07-1099>.
46. Sarafidis PA, Tsapas A. Empagliflozin, Cardiovascular outcomes, and mortality in type 2 diabetes. *N Engl J Med.* 2016;374:1092. <https://doi.org/10.1056/NEJMc1600827>.
47. Durante W, Behnammanesh G, Peyton KJ. Effects of Sodium-glucose cotransporter 2 inhibitors on vascular cell function and arterial remodeling. *Int J Mol Sci.* 2021;22. <https://doi.org/10.3390/ijms22168786>.
48. Solini A, Giannini L, Seghieri M, Vitolo E, Taddei S, Ghiadoni L, Bruno RM. Dapagliflozin acutely improves endothelial dysfunction, reduces aortic stiffness and renal resistive index in type 2 diabetic patients: a pilot study. *Cardiovasc Diabetol.* 2017;16:138. <https://doi.org/10.1186/s12933-017-0621-8>.
49. Ellulu MS, Patimah I, Khaza'ai H, Rahmat A, Abed Y. Obesity and inflammation: the linking mechanism and the complications. *Arch Med Sci.* 2017;13:851–63. <https://doi.org/10.5114/aoms.2016.58928>.
50. McMurray JJV, Solomon SD, Inzucchi SE, Køber L, Kosiborod MN, Martinez FA, Ponikowski P, Sabatine MS, Anand IS, Bøhlhøve J, et al. Dapagliflozin in patients with heart failure and reduced ejection fraction. *N Engl J Med.* 2019;381:1995–2008. <https://doi.org/10.1056/NEJMoa1911303>.
51. Manning BD, Toker A. AKT/PKB signaling: navigating the network. *Cell.* 2017;169:381–405. <https://doi.org/10.1016/j.cell.2017.04.001>.
52. Manning BD, Cantley LC. AKT/PKB signaling: navigating downstream. *Cell.* 2007;129:1261–74. <https://doi.org/10.1016/j.cell.2007.06.009>.
53. Engelman JA, Luo J, Cantley LC. The evolution of phosphatidylinositol 3-kinases as regulators of growth and metabolism. *Nat Rev Genet.* 2006;7:606–19. <https://doi.org/10.1038/nrg1879>.
54. Vanhaesebroeck B, Guillermet-Guibert J, Graupera M, Bilanges B. The emerging mechanisms of isoform-specific PI3K signalling. *Nat Rev Mol Cell Biol.* 2010;11:329–41. <https://doi.org/10.1038/nrm2882>.
55. Morrison DK. MAP kinase pathways. *Cold Spring Harb Perspect Biol.* 2012;4. <https://doi.org/10.1101/cshperspect.a011254>.
56. Kyriakis JM, Avruch J. Mammalian MAPK signal transduction pathways activated by stress and inflammation: a 10-year update. *Physiol Rev.* 2012;92:689–737. <https://doi.org/10.1152/physrev.00028.2011>.
57. Takeuchi O, Akira S. Pattern recognition receptors and inflammation. *Cell.* 2010;140:805–20. <https://doi.org/10.1016/j.cell.2010.01.022>.
58. Shin EJ, Tran HQ, Nguyen PT, Jeong JH, Nah SY, Jang CG, Nabeshima T, Kim HC. Role of Mitochondria in Methamphetamine-Induced Dopaminergic Neurotoxicity: involvement in oxidative stress, Neuroinflammation, and Proapoptosis-a Review. *Neurochem Res.* 2018;43:66–78. <https://doi.org/10.1007/s11064-017-2318-5>.
59. Cybulsky MI, Gimbrone MA Jr. Endothelial expression of a mononuclear leukocyte adhesion molecule during atherogenesis. *Science.* 1991;251:788–91. <https://doi.org/10.1126/science.1990440>.
60. Ley K, Laudanna C, Cybulsky MI, Nourshargh S. Getting to the site of inflammation: the leukocyte adhesion cascade updated. *Nat Rev Immunol.* 2007;7:678–89. <https://doi.org/10.1038/nri2156>.
61. Zinman B, Wanner C, Lachin JM, Fitchett D, Bluhmki E, Hantel S, Mattheus M, Devins T, Johansen OE, Woerle HJ, et al. Empagliflozin, Cardiovascular outcomes, and mortality in type 2 diabetes. *N Engl J Med.* 2015;373:2117–28. <https://doi.org/10.1056/NEJMoa1504720>.
62. Cherney DZ, Perkins BA, Soleymanlou N, Maione M, Lai V, Lee A, Fagan NM, Woerle HJ, Johansen OE, Broedl UC, et al. Renal hemodynamic effect of sodium-glucose cotransporter 2 inhibition in patients with type 1 diabetes mellitus. *Circulation.* 2014;129:587–97. <https://doi.org/10.1161/circulationaha.113.005081>.
63. Balmaceda-Aguilera C, Cortés-Campos C, Cifuentes M, Peruzzo B, Mack L, Tapia JC, Oyarce K, García MA, Nualart F. Glucose transporter 1 and monocarboxylate transporters 1, 2, and 4 localization within the glial cells of shark blood-brain-barriers. *PLoS ONE.* 2012;7:e32409. <https://doi.org/10.1371/journal.pone.0032409>.
64. Zhou Y, Tai S, Zhang N, Fu L, Wang Y. Dapagliflozin prevents oxidative stress-induced endothelial dysfunction via sirtuin 1 activation. *Biomed Pharmacother.* 2023;165:115213. <https://doi.org/10.1016/j.biopha.2023.115213>.
65. de Almeida A, de Almeida Rezende MS, Dantas SH, de Lima Silva S, de Oliveira J Lourdes Assunção Araújo, de Azevedo F, Alves R, de Menezes GMS, Dos Santos PF, Gonçalves TAF et al. (2020) Unveiling the Role of Inflammation and Oxidative Stress on Age-Related Cardiovascular Diseases. *Oxid Med Cell Longev* 2020:1954398. <https://doi.org/10.1155/2020/1954398>
66. Thomas TP, Grisanti LA. The dynamic interplay between cardiac inflammation and fibrosis. *Front Physiol.* 2020;11:529075. <https://doi.org/10.3389/fphys.2020.529075>.
67. Tran N, Garcia T, Aniqi M, Ali S, Ally A, Nauli SM. Endothelial nitric oxide synthase (eNOS) and the Cardiovascular System: in physiology and in Disease States. *Am J Biomed Sci Res.* 2022;15:153–77.
68. Zhang H, Park Y, Wu J, Chen X, Lee S, Yang J, Dellsparger KC, Zhang C. Role of TNF-alpha in vascular dysfunction. *Clin Sci (Lond).* 2009;116:219–30. <https://doi.org/10.1042/cs20080196>.
69. Merovci A, Mari A, Solis-Herrera C, Xiong J, Daniele G, Chavez-Velazquez A, Tripathy D, Urban McCarthy S, Abdul-Ghani M, DeFronzo RA. Dapagliflozin lowers plasma glucose concentration and improves  $\beta$ -cell function. *J Clin Endocrinol Metab.* 2015;100:1927–32. <https://doi.org/10.1210/jc.2014-3472>.

70. Shyr ZA, Yan Z, Ustione A, Egan EM, Remedi MS. SGLT2 inhibitors therapy protects glucotoxicity-induced  $\beta$ -cell failure in a mouse model of human KATP-induced diabetes through mitigation of oxidative and ER stress. *PLoS ONE*. 2022;17:e0258054. <https://doi.org/10.1371/journal.pone.0258054>.
71. Neal B, Perkovic V, Mahaffey KW, de Zeeuw D, Fulcher G, Erondu N, Shaw W, Law G, Desai M, Matthews DR. Canagliflozin and Cardiovascular and renal events in type 2 diabetes. *N Engl J Med*. 2017;377:644–57. <https://doi.org/10.1056/NEJMoa1611925>.
72. He X, Yuan D. A review regarding the article 'Targeting inflammatory signaling pathways with SGLT2 inhibitors: insights into cardiovascular health and cardiac cell improvement'. *Curr Probl Cardiol*. 2024;49:102563. <https://doi.org/10.1016/j.cpcardiol.2024.102563>.
73. Pagliuca FW, Millman JR, Gürtler M, Segel M, Van Dervort A, Ryu JH, Peterson QP, Greiner D, Melton DA. Generation of functional human pancreatic  $\beta$  cells in vitro. *Cell*. 2014;159:428–39. <https://doi.org/10.1016/j.cell.2014.09.040>.
74. Tandy N, Irwin N, Flatt PR, Moffett RC. Dapagliflozin exerts positive effects on beta cells, decreases glucagon and does not alter beta- to alpha-cell transdifferentiation in mouse models of diabetes and insulin resistance. *Biochem Pharmacol*. 2020;177:114009. <https://doi.org/10.1016/j.bcp.2020.114009>.
75. Karlsson D, Ahnmark A, Sabirsh A, Andréasson AC, Gennemark P, Sandinge AS, Chen L, Tyrberg B, Lindén D, Sörhede Winzell M. (2022) Inhibition of SGLT2 preserves function and promotes proliferation of human islets cells in vivo in diabetic mice. *Biomedicines* 10. <https://doi.org/10.3390/biomedicines10020203>
76. Aguayo-Mazzucato C, Koh A, El Khattabi I, Li WC, Toschi E, Jermendy A, Juhl K, Mao K, Weir GC, Sharma A, et al. MafA expression enhances glucose-responsive insulin secretion in neonatal rat beta cells. *Diabetologia*. 2011;54:583–93. <https://doi.org/10.1007/s00125-010-2026-z>.
77. Kataoka K, Han SI, Shioda S, Hirai M, Nishizawa M, Handa H. MafA is a glucose-regulated and pancreatic beta-cell-specific transcriptional activator for the insulin gene. *J Biol Chem*. 2002;277:49903–10. <https://doi.org/10.1074/jbc.M206796200>.
78. Zhang DD. Mechanistic studies of the Nrf2-Keap1 signaling pathway. *Drug Metab Rev*. 2006;38:769–89. <https://doi.org/10.1080/03602530600971974>.
79. Cross DA, Alessi DR, Cohen P, Andjelkovich M, Hemmings BA. Inhibition of glycogen synthase kinase-3 by insulin mediated by protein kinase B. *Nature*. 1995;378:785–9. <https://doi.org/10.1038/378785a0>.
80. Hotamisligil GS. Endoplasmic reticulum stress and the inflammatory basis of metabolic disease. *Cell*. 2010;140:900–17. <https://doi.org/10.1016/j.cell.2010.2.034>.
81. Arthur JS, Ley SC. Mitogen-activated protein kinases in innate immunity. *Nat Rev Immunol*. 2013;13:679–92. <https://doi.org/10.1038/nri3495>.
82. Fu S, Yang L, Li P, Hofmann O, Dicker L, Hide W, Lin X, Watkins SM, Ivanov AR, Hotamisligil GS. Aberrant lipid metabolism disrupts calcium homeostasis causing liver endoplasmic reticulum stress in obesity. *Nature*. 2011;473:528–31. <https://doi.org/10.1038/nature09968>.
83. Chen D, Cao D, Sui P. Tetramethylpyrazine relieves LPS-induced pancreatic  $\beta$ -cell Min6 injury via regulation of miR-101/MKP-1. *Artif Cells Nanomed Biotechnol*. 2019;47:2545–52. <https://doi.org/10.1080/21691401.2019.1628039>.
84. Zhou Y, Zhang Y, Wang J. Trefoil Factor 2 regulates proliferation and apoptosis of pancreatic Cancer cells and LPS-Induced Normal Pancreatic Duct cells by  $\beta$ -Catenin pathway. *Cancer Manag Res*. 2020;12:10705–13. <https://doi.org/10.2147/cmar.S274578>.
85. John A, Raza H. Alterations in inflammatory cytokines and Redox Homeostasis in LPS-Induced pancreatic Beta-cell toxicity and mitochondrial stress: Protection by Azadirachtin. *Front Cell Dev Biol*. 2022;10:867608. <https://doi.org/10.3389/fcell.2022.867608>.
86. Ku CW, Ho TJ, Huang CY, Chu PM, Ou HC, Hsieh PL. Cordycepin attenuates Palmitic Acid-Induced inflammation and apoptosis of vascular endothelial cells through mediating PI3K/Akt/eNOS signaling pathway. *Am J Chin Med*. 2021;49:1703–22. <https://doi.org/10.1142/s0192415x21500804>.
87. Dyck JRB, Sossalla S, Hamdani N, Coronel R, Weber NC, Light PE, Zuurbier CJ. Cardiac mechanisms of the beneficial effects of SGLT2 inhibitors in heart failure: evidence for potential off-target effects. *J Mol Cell Cardiol*. 2022;167:17–31. <https://doi.org/10.1016/j.yjmcc.2022.03.005>.
88. Packer M. Activation and inhibition of Sodium-Hydrogen Exchanger is a mechanism that links the pathophysiology and treatment of diabetes Mellitus with that of heart failure. *Circulation*. 2017;136:1548–59. <https://doi.org/10.1161/circulationaha.117.030418>.
89. Pfaffenbach KT, Lee AS. The critical role of GRP78 in physiologic and pathologic stress. *Curr Opin Cell Biol*. 2011;23:150–6. <https://doi.org/10.1016/j.ccb.2010.09.007>.
90. Li J, Lee AS. Stress induction of GRP78/BiP and its role in cancer. *Curr Mol Med*. 2006;6:45–54. <https://doi.org/10.2174/156652406775574523>.
91. Kaufman RJ. Orchestrating the unfolded protein response in health and disease. *J Clin Invest*. 2002;110:1389–98. <https://doi.org/10.1172/jci16886>.
92. Wang FZ, Wei WB, Li X, Huo JY, Jiang WY, Wang HY, Qian P, Li ZZ, Zhou YB. The cardioprotective effect of the sodium-glucose cotransporter 2 inhibitor dapagliflozin in rats with isoproterenol-induced cardiomyopathy. *Am J Transl Res*. 2021;13:10950–61.
93. Yeoh SE, Docherty KF, Campbell RT, Jhund PS, Hammarstedt A, Heerspink HJL, Jarolim P, Køber L, Kosiborod MN, Martinez FA, et al. Endothelin-1, outcomes in patients with heart failure and reduced ejection fraction, and effects of Dapagliflozin: findings from DAPA-HF. *Circulation*. 2023;147:1670–83. <https://doi.org/10.1161/circulationaha.122.063327>.
94. Tian J, Zhang M, Suo M, Liu D, Wang X, Liu M, Pan J, Jin T, An F. Dapagliflozin alleviates cardiac fibrosis through suppressing EndMT and fibroblast activation via AMPK $\alpha$ /TGF- $\beta$ /Smad signalling in type 2 diabetic rats. *J Cell Mol Med*. 2021;25:7642–59. <https://doi.org/10.1111/jcmm.16601>.
95. Uthman L, Baartscheer A, Schumacher CA, Fiolet JWT, Kuschma MC, Holmann MW, Coronel R, Weber NC, Zuurbier CJ. Direct cardiac actions of Sodium glucose cotransporter 2 inhibitors Target pathogenic mechanisms underlying heart failure in Diabetic patients. *Front Physiol*. 2018;9:1575. <https://doi.org/10.3389/fphys.2018.01575>.
96. Sun HJ, Wu ZY, Nie XW, Bian JS. Role of endothelial dysfunction in Cardiovascular diseases: the Link between inflammation and hydrogen sulfide. *Front Pharmacol*. 2019;10:1568. <https://doi.org/10.3389/fphar.2019.01568>.
97. Baaten C, Vondenhoff S, Noels H. Endothelial cell dysfunction and increased Cardiovascular risk in patients with chronic kidney disease. *Circ Res*. 2023;132:970–92. <https://doi.org/10.1161/circresaha.123.321752>.
98. Allbritton-King JD, García-Cardena G. Endothelial cell dysfunction in cardiac disease: driver or consequence? *Front Cell Dev Biol*. 2023;11:1278166. <https://doi.org/10.3389/fcell.2023.1278166>.
99. Nguyen T, Nioi P, Pickett CB. The Nrf2-antioxidant response element signaling pathway and its activation by oxidative stress. *J Biol Chem*. 2009;284:13291–5. <https://doi.org/10.1074/jbc.R900010200>.

## Publisher's note

Springer Nature remains neutral with regard to jurisdictional claims in published maps and institutional affiliations.